An explanation for the isotopic offset between soil and stem water in a temperate tree species

Adrià Barbeta[1,2*], Teresa E. Gimeno[1,3,4], Laura Clavé[1], Bastien Fréjaville[1], Sam P. Jones[1,5], Camille Delvigne[1,6], Lisa Wingate[1], Jérôme Ogée[1]

[1] INRAE, UMR1391 ISPA, 33140 Villenave d'Ornon, France
[2] BEECA, Universitat de Barcelona, 08028 Barcelona, Catalonia, Spain
[3] Basque Centre for Climate Change, 48940 Leioa, Spain
[4] IKERBASQUE, Basque Foundation for Science, 48008, Bilbao, Spain
[5] Instituto Nacional de Pesquisas da Amazônia, Manaus CEP 69060-001, Brazil
[6] Université catholique de Louvain, 1348 Louvain-la-Neuve, Belgium
* Correspondence to: Adrià Barbeta (adria.barbeta.margarit@gmail.com) and Jérôme Ogée (jerome.ogee@inrae.fr)

Summary (maximum 200 words)

- A growing number of field studies report isotopic offsets between stem water and its potential sources that prevent the unambiguous identification of plant water origin using water isotopes. We explored the causes of this isotopic offset by conducting a controlled experiment on the temperate tree species *Fagus sylvatica*.
- We measured δ^2H and $\delta^{18}O$ of soil and stem water from potted saplings growing on three soil substrates and subjected to two watering regimes.
- Regardless of substrate, soil and stem water δ^2H were similar only near permanent wilting point. Under moister conditions, stem water δ^2H was 11±3‰ more negative than soil water δ^2H, coherent with field studies. Under drier conditions, stem water δ^2H became progressively more enriched than soil water δ^2H. Although stem water $\delta^{18}O$ broadly reflected that of soil water, soil-stem δ^2H and $\delta^{18}O$ differences were correlated ($r = 0.76$) and increased with transpiration rates indicated by proxies.
- Soil-stem isotopic offsets are more likely caused by water isotope heterogeneities within the soil pore and stem tissues, which would be masked under drier conditions due to evaporative

enrichment, than by fractionation under root water uptake. Our results challenge our current understanding of isotopic signals in the soil-plant continuum.

Keywords: ecohydrology, root water uptake, water isotopes, plant water sources, *Fagus sylvatica*

Total word count: 6480

- Introduction: 2175
- Material and methods: 1670
- Results: 1025
- Discussion: 1602
- Acknowledgements: 118

References: 60

Tables: 1.

Figures: 8 (Figs. from 1 to 8 in colour).

Supporting Information: 11 Figures and 1 Note.

1. Introduction

Plant transpiration is the main flux returning water from the land surface to the atmosphere (Jasechko *et al.*, 2013) emphasising the importance of vegetation in the global water cycle. To trace variations in land-atmosphere water fluxes it is necessary to identify the water pools accessed by plants and how these change over time and space. Analysis of the natural abundance of stable isotopes in water is a commonly used technique for this purpose (Dawson & Ehleringer, 1991; Barbeta & Peñuelas, 2017). This technique is usually applied under the assumption that no isotopic fractionation occurs during root water uptake, as suggested by a series of early observations conducted on plants grown hydroponically (Washburn & Smith, 1934; Zimmermann *et al.*, 1967). Although hydroponic systems do not have the mechanistic complexity and heterogeneity of natural systems (Penna *et al.*, 2018), the evidence for root water uptake not fractionating paved the way for using water stable isotopes to infer plant water sources (White *et al.*, 1985; Dawson & Ehleringer, 1991), assess their spatiotemporal variability (Bertrand *et al.*, 2014; Barbeta *et al.*, 2015) and their ecological implications (Moreno-Gutiérrez *et al.*, 2012; De Deurwaerder *et al.*, 2018).

Improvements in the capability for higher throughput using modern water extraction and isotopic determination techniques have helped collect water isotopic datasets that are more comprehensive than ever before (Stumpp *et al.*, 2018). Perhaps more importantly, plant water source studies are no longer restricted to either oxygen ($\delta^{18}O$) or hydrogen ($\delta^{2}H$) isotopic composition, but routinely present data for both isotopes. An emerging feature of studies using dual-isotope approaches is that oxygen and hydrogen isotopes do not always agree in the attribution of the source(s) of plant water. This is caused by isotopic offsets between stem water and all potential water sources, that is, the isotopic composition of stem water does not match any of the considered sources in the dual-isotope space. These isotopic offsets have been observed in field sites encompassing a wide range of soil types and biomes, including semi-arid shrublands (Wang *et al.*, 2017), conifer forests (Geris *et al.*, 2017 Brooks *et al.*, 2010), broad-leaved forests (Goldsmith *et al.*, 2018; Barbeta *et al.*, 2019 Bowling *et al.*, 2017), urban gardens (Oerter and Bowen, 2017), tropical rainforests (Brum *et al.*, 2018; De Deurwaerder *et al.*, 2018) and rice paddy fields (Mahindawansha *et al.*, 2018). In such cases, the use of oxygen or hydrogen isotopes separately can lead to significantly different attributions of plant water sources

(Lin & Sternberg, 1993; Evaristo *et al.*, 2017; Brum *et al.*, 2018; Barbeta *et al.*, 2019). Some authors acknowledged this caveat and used either δ^2H or $\delta^{18}O$ to infer plant water sources, or proposed and discussed potential mechanisms and implications (Bowling *et al.*, 2017; Evaristo *et al.*, 2017; Barbeta *et al.*, 2019; Oerter & Bowen, 2019; Oerter *et al.*, 2019). However, in many cases, soil-stem isotopic offsets are not addressed.

An isotopic offset between stem water and all potential water sources cannot be attributed solely to methodological issues. For example, contamination of soil- or plant-extracted water by organic compounds can bias measurements of the stable isotopes in water, especially when using laser-based instruments (e.g. Schultz *et al.*, 2011; Martín-Gómez *et al.*, 2015; Millar *et al.*, 2018). However, these contaminations are now routinely dealt with using custom, post-measurement corrections and are unlikely to cause a systematic bias since (1) isotopic offsets have been found in studies using both mass spectrometers (Brooks *et al.*, 2010; Bowling *et al.*, 2017; Brum *et al.*, 2018; Goldsmith *et al.*, 2018) and laser-based instruments (Geris *et al.*, 2017; Barbeta *et al.*, 2019; De Deurwaerder *et al.*, 2018) and (2) both types of analysers render similar and reproducible results on the same soil water samples (Orlowski *et al.*, 2018). Additional confounding effects related to water extraction techniques should not be overlooked (Thorburn *et al.*, 1993; Walker *et al.*, 1994; Millar *et al.*, 2015; Orlowski *et al.*, 2018). For example, cryogenic vacuum extraction (CVE), is the most widely used technique nowadays but has been shown to give results sensitive to many parameters such as soil texture, water content, extraction time or temperature (Orlowski *et al.*, 2018). Alternative soil and stem water extraction techniques exist (Wassenaar *et al.*, 2008; Munksgaard *et al.*, 2014) and comparative studies often concluded that contrasting results were caused by differences in extraction yields affecting the isotopic composition of the extracted water of soil (Walker *et al.*, 1994) and stem (Thorburn *et al.*, 1993) *via* Rayleigh distillation processes, or by large differences in organic contamination of the extracted water (Millar *et al.*, 2015). However, if well conducted, water extraction techniques such as CVE lead to extraction yields >99% and low levels of organic contamination (Orlowski *et al.*, 2013; Millar *et al.*, 2015). Another possibility explaining soil-stem isotopic offsets is that the pools of water extracted vary with different techniques, even though some of these pools might be less relevant to the study of plant water sources (e.g. water adsorbed on soil particles or plant storage water). For example, a recent study on wheat showed that the soil-stem isotopic offset was reduced when using direct vapour equilibration on stems, compared to CVE (Millar *et*

al., 2018). Unfortunately, for woody species, direct vapour equilibration presents additional problems related to the interference of volatile organic compounds during isotopic determination and still needs further development and testing (Volkmann et al. 2016; Raulerson, 2019). Regardless of the technique, a consistent pattern is observed frequently across studies whereby stem water generally plots below and to the right of any considered water source in the dual isotope "space" (i.e., a graphical representation of δ^2H *vs*. $\delta^{18}O$ values) (Brooks *et al.*, 2010). Such a systematic pattern is unlikely to be attributed solely to soil and stem water extraction artefacts but it remains to be tested whether it is reproducible under controlled conditions.

Isotopic offsets between source and stem water have now been reported in ecologically diverse plant species, but was firstly observed in halophytic and xerophytic plants (Lin & Sternberg, 1993; Ellsworth & Williams, 2007). These drought and salinity tolerant plants have a highly developed Casparian strip on the radial cell walls of the root endodermis that impedes apoplastic movement of water, forcing water to move symplastically across cell membranes (Ellsworth & Williams, 2007 and references therein). Water movement through the symplastic route has been hypothesized to fractionate hydrogen isotopes in water, leading to a 3-9‰ depletion of stem water compared to soil water in halophytic and xerophytic plants (Lin & Sternberg, 1993; Ellsworth & Williams, 2007). More recently, Poca *et al.*, (2019) showed that arbuscular mycorrhizal associations enhanced the isotopic offset between soil and stem water (up to -15‰) in potted seedlings of the xerophytic species *Acacia caven*. They proposed that isotopic fractionation occurred during trans-membrane water transport *via* aquaporins, and that this mode of transport must be enhanced in presence of mycchorizal associations. However, the impairment of the apoplastic pathway was not demonstrated in this study. More importantly, this mechanism cannot explain why other studies, including our own results from a temperate deciduous forest (Barbeta *et al.*, 2019), found similar isotopic offsets (a soil water excess of 8.4‰) in plant species where root water uptake through the apoplastic route should not be impeded.

It is also increasingly recognised that soil water may exhibit pore-scale isotopic heterogeneity created by water-surface interaction effects that leads to an isotopic depletion of adsorbed water compared to bulk soil water (Oerter *et al.*, 2014; Chen *et al.*, 2016; Lin & Horita, 2016; Lin *et al.*, 2018; Penna *et al.*, 2018; Oerter & Bowen, 2019). Then, a depletion of stem water compared to bulk soil water could indicate that trees take up water adsorbed onto soil particles. However,

we would expect roots to take up the most mobile (i.e. gravimetric and capillary) soil water (see the discussion in Bowling *et al.*, 2017) which, in contrast to adsorbed water, should be more enriched than bulk soil water (Chen *et al.*, 2016; Barbeta *et al.*, 2019). Under low water availability and high evaporative demand, it has also been shown that stem water loss *via* evaporation can create significant isotopic enrichment of stem water (Bowling *et al.*, 2017; Martín-Gómez *et al.*, 2017) further complicating the inference of plant water sources from stem water's isotopic composition. Although such evaporative enrichment of stem water should be easily detectable in the dual-isotope space and is a process that needs to be considered when attempting to derive plant water sources, it cannot explain why stem water is more depleted in δ^2H than any considered water source.

Isotopic heterogeneity in plant water pools was further proposed by Zhao *et al.* (2016) as an alternative explanation for the observed soil-stem water isotopic offsets. They directly extracted sap (i.e. vessel water) from stems of the desert riparian trees *Populus euphratica* and found that its isotopic composition matched that of groundwater. On the other hand, total water from stem or root samples was systematically depleted in ^2H with respect to sap water and all other likely water sources. They attributed this observation to a putative discrimination during water transport and redistribution within the plant. Unfortunately, repeating this experiment with other species or during the dry season is very challenging, as it requires the xylem sap to be under positive pressure to be collected. Only indirect evidence can be deducted, once all other hypotheses have been discarded.

In this context, we conducted a glasshouse experiment with potted saplings of a temperate deciduous tree (European beech, *Fagus sylvatica* L.) to quantify potential isotopic offsets between plant and source water and to elucidate how these vary with water availability, soil properties and plant physiological performance. We chose this temperate tree species because it had been shown in a previous field study that isotopic separation between source and xylem water was likely (Barbeta *et al.*, 2019). In the field, the total extension of the root system is difficult to assess so the presence of unconsidered water sources can never be completely ruled out (Barbeta *et al.*, 2019; Oerter & Bowen, 2019). In contrast, the advantage of potted plants is that the actual water source can be characterized more thoroughly. We thus wanted to verify that the isotopic offsets observed in the field between xylem and soil water were reproducible under

controlled conditions. Our experimental design builds up on the hypotheses formulated by previous studies (Zhao *et al.*, 2016; Martín-Gómez *et al.*, 2017; Vargas *et al.*, 2017; Barbeta *et al.*, 2019; Oerter & Bowen, 2019) and more importantly, expands the range of soil water availabilities tested to date. The isotopic offset between soil and stem water reported by Vargas *et al.* (2017) was based on a glasshouse experiment with potted *Persea americana* saplings subjected to a relatively mild water shortage (matching the study species demands) on two contrasting soil types. Here we not only explored much harsher water shortages, but we also complemented our experiment with a control treatment whereby plants were regularly watered throughout the experiment to maintain the soil at field capacity. By doing so, we were revisiting the early hydroponic experiments at the origin of the idea that root water uptake is a non-fractionating process, while adding the complexity of textured soils. After several weeks of regular irrigation to compensate for water losses, fractionation during root water uptake (noted ε_U in Fig. 1A) should lead to an isotopic enrichment of soil water above irrigation water ($\delta_{soil} = \delta_P + \varepsilon_U$) while stem water should arrive at isotopic steady state and reflect exactly the isotopic composition of irrigation water ($\delta_{soil} = \delta_P$), leading to a constant isotopic offset between bulk soil and stem waters (Fig 1A). If soil evaporation is not fully suppressed, soil water will become slightly more enriched than $\delta_P + \varepsilon_U$ but the isotopic difference between soil and stem water should not differ (see Notes S1). Pore-scale isotopic heterogeneity in soil and xylem water pools may be an alternative explanation for the observed soil-xylem isotopic offsets (Fig. 1B). Under well-watered conditions, the adsorbed soil water would represent a small fraction (f_a) of total soil water and thus the isotopic composition of bulk soil water (δ_{soil}) would resemble that of irrigation water (δ_P). In turn, the isotopic composition of bulk stem water (δ_{stem}) would still be more depleted than δ_{soil} (and δ_P) because of isotopic heterogeneity within the stem (i.e. isotopic differences between vessel/sap water and water in non-conductive tissues, Zhao et al., 2016). This would imply that these non-conductive tissues are depleted compared to sap water, since sap would have the signal of the water taken up (δ_P) (Fig. 1B). To test further this alternative situation, we also used three soil textures, including one containing rock fragments, to play on the fraction of adsorbed water in soils and help disentangle the separate roles of soil water content and water potential on the isotopic offsets. To sum up, our aim was to (i) test whether isotopic offsets between stem water and their sources were reproducible in potted plants with a

unique source of water and (ii) identify the soil physical and/or plant physiological mechanisms producing these isotopic offsets.

2. Material and Methods

2.1 Plant material and experimental design

From February to July 2018 we grew saplings of *F. sylvatica* in a temperature-controlled glasshouse (Talence, France). Climatic conditions inside the glasshouse were monitored with a temperature and humidity probe (HMP60, Vaisala, Vanta, Finland) and a quantum sensor (SQ200, Apogee, Logan, UT, US). Over the study period (14 May to 20 June 2018, n = 38 days), mean air temperature inside the glasshouse (±SE) was 20 ± 0.3 °C during the day and 16.3 ± 0.2 °C at night. A shading cloth was permanently deployed from 24 April 2018 and mean daily photosynthetic photon flux density (PPFD) was 10 ± 0.9 mol m^{-2} d^{-1}.

One-year old beech saplings (mean diameter of 2.1±0.5 cm) were obtained from a commercial nursery (Naudet pépinières, Leuglay, France) grown from seeds originating from the Armorican massif (Bretagne, NE France). On 20 February 2018, we transplanted 220 plants into 3.5 L squared pots filled with three soil types. The three soil types consisted of a volume mix of (1) soil:sand:commercial substrate (2:1:1), (2) soil:sand:commercial substrate:crushed rocks (10:5:5:1) and (3) soil:sand:commercial substrate:clay (10:2:5:3). Substrates were: sandy soil from a nearby pine plantation (Jones *et al.*, 2017) (Cestas, France), with a total organic C of 33 g kg^{-1} and a total N < 1 g kg^{-1} ; washed river sand (Gedimat, Levallois-Perret, France); commercial peat substrate for plant growth (“Terrau Gazon”, Soufflet Vigne, Martillac, France); crushed rocks obtained from oven-dried (48 h at 105 °C) limestone rocks collected near the Ciron river (Pompéjac, France) and commercial soil conditioner (bentonite clay, Magellan-bio.fr, Cysoing, France). According to texture analyses, the first and second (without the rocks) soil types were classified as coarse sand and the third type was a sandy loam in the limit of sandy clay loam, henceforth sandy clay loam. Soil water retention curves estimated from pedotransfer functions (R package *soilwater*) are presented in Fig. S1. We transplanted 100 plants onto the coarse sandy soil, 60 plants onto the coarse sandy soil with rocks and 60 plants onto the sandy clay loam.

From February 2018 until 13 May 2018 all pots were watered regularly to field capacity with tap water (δ^2H = -35.33 ± 0.25 and $\delta^{18}O$ = -5.90 ± 0.3) and soil water was allowed to freely evaporate from the surface. Starting on 14 May 2018, we watered all pots daily to field capacity for three consecutive days to ensure a homogeneous soil water pool in each pot. A set of 12 plants from each soil type continued to be watered to field capacity regularly (control treatment), while watering was withheld for all other plants from the 17 May 2018 until the end of the drying experiment on 20 June 2018 (drought treatment). A plastic top was placed on all pots to reduce soil water evaporation on 17 May 2018. Mean soil gravimetric water content (GWC) over time for each treatment and soil type was calculated from the weights of ten and five pots for the drought and control treatments, respectively, for each soil type. Individual GWC and plant water contents for sampled pots and plants were estimated from the soil and stem samples used for cryogenic vacuum distillation. GWC was then converted to volumetric water content (VWC) using the bulk density of each soil type. Based on the retention curve of each soil type, we determined the VWC corresponding to the permanent wilting point (VWC at which soil matric potential is -1500 kPa). For each sampled pot, we calculated θ_{rel}, the difference between the VWC of a given pot minus the VWC at permanent wilting point. Thus, positives θ_{rel} values corresponded to conditions in which soil water can be taken up by roots whilst negative values imply that soil water is not extractable by the plant.

In addition to the two watering treatments, we applied a low vapour pressure deficit (VPD) treatment during the first two sampling campaigns on a subset of plants from the drought treatment with the rock-free coarse sandy soil. This treatment consisted of covering five plants with a semi-transparent plastic bag the evening before the day of sampling. The aim was to reduce transpiration for individual plants over the course of one day to assess its impact on potential isotopic offsets between soil and stem water pools.

2.2 Ecophysiological measurements and destructive harvests

Over the course of the drying experiment, we performed five campaigns of ecophysiological measurements and destructive harvests for water isotope analysis (1, 8, 15, 28 and 35 days after the last watering event of the drought treatment on 17 May 2018). On each campaign and each soil type, we harvested three plants from the control and five from the drought treatment, except on the first and second campaigns, where five additional plants from the low VPD treatment (on

253 rock-free sandy soil) were also sampled. For each pot, a soil core from the surface to the bottom
254 of the pot was taken, homogenised in a clean plastic tray and sub-sampled for isotopic analysis.
255 For each plant we cut two 5cm-long lignified segments, one from the root and one from the stem
256 (separated by at least 2.5 cm below the aboveground stem) and peeled off the bark and phloem.
257 Soil, root and stem samples were rapidly transferred into screw-cap glass vials, sealed with
258 Parafilm® and stored in a cool box until transported to the laboratory where they were stored at
259 4°C until further analysis.

260 The day of each destructive harvest (conducted in early afternoon), ecophysiological
261 measurements were also performed on leaves from the harvested plants and included
262 measurements of stomatal conductance to water vapour (g_s) and leaf water potential at predawn
263 (Ψ_{pd}) and midday (Ψ_{md}). Leaf water potential was measured with a custom-made Scholander
264 type chamber (DG Meca, Gradignan, France) on one leaf per plant. Stomatal conductance was
265 measured at mid-morning (10:30-11:30, local time) with two cross-calibrated handheld
266 porometers (SC-1 Leaf Porometer, Decagon Inc., Pullman, WA, US) on one leaf per plant. On
267 the second campaign, we measured g_s with the two handheld porometers and with an infrared gas
268 analyser (IRGA, LI-COR 6400, LI-COR, Lincoln, NE, US), on the same leaves and matching the
269 conditions inside the gas exchange chamber (temperature, humidity, PPFD and CO_2
270 concentration) to those prevailing in the glasshouse. The significant correlation between g_s
271 measurements showed that measurements from the handheld porometers neither overestimated
272 nor underestimated stomatal conductance compared to the IRGA ($p = 0.001$, $R^2 = 0.45$, slope:
273 1.03 ± 0.25).

274 *2.3 Cryogenic water extraction and analyses of water isotopic composition*

275 The extraction of water from soil, stem, root and rock samples was performed by cryogenic
276 vacuum distillation using a design and methodology proposed by Orlowski *et al.* (2013), as
277 described in Jones *et al.* (2017). At the onset of the extraction, up to 24 samples kept in sampling
278 glass vials were inserted in larger extraction glass vials connected to a vacuum extraction line
279 and frozen in liquid nitrogen. The extraction line was then evacuated down to an atmospheric
280 (static) pressure of less than 1 Pa and composed of 24 glass U-shape tubes that were then
281 inserted in liquid nitrogen to create a cold trap. Samples were then immersed in a water bath at
282 ambient temperature, and the water bath was gradually heated up to 80°C (within 1h) to start the

distillation process. Samples remained in the heated bath at 80°C for 2.5h. Pressure in the extraction line was continuously monitored with sub-atmospheric pressure sensors (APG100 Active Pirani Vacuum Gauges, Edwards, Burgess Hill, UK) to check that the lines remained leak-tight throughout the entire extraction and that the water extraction had ended. Samples were weighed before and after the extraction and before and after being oven-dried for 24h at 105°C to assess extraction efficiency. GWC was estimated from each sample by using the weight measured before and after the cryogenic extraction and again after oven-drying (Newberry *et al.*, 2017).

The isotopic composition (δ^2H and $\delta^{18}O$) of the extracted waters was measured with an off-axis integrated cavity optical spectrometer (TIWA-45EP, Los Gatos Research, USA) coupled to a liquid auto-sampler and vaporiser (LC-xt, PAL systems, Switzerland). All isotopic data reported here are calibrated using two internal standards and expressed on the VSMOW-SLAP scale, as described in Jones *et al.* (2017). Because the presence of organic compounds (ethanol, methanol and/or other biogenic volatile compounds) in water samples can lead to large isotopic discrepancies in laser-based analyses (Martín-Gómez *et al.*, 2015; Wassenaar et al. 2018), we developed a post-correction algorithm for the presence of organic compounds based on the narrowband (for methanol) and broadband (for ethanol) metrics of the absorption spectra (Brian Leen *et al.*, 2012). Post-corrections relating how these metrics affect the isotopic composition of waters contaminated with known amounts of ethanol and methanol were developed specifically for our instrument. Overall, these post-corrections were usually higher for stem water than for meteoric or soil water samples but always remained quite small (i.e. below 1.5 ‰ for δ^2H and below 0.7 ‰ for $\delta^{18}O$).

2.4 Data analyses

Statistical analysis was conducted in R (R Core Team, 2019) using either general linear models (GLM) or generalized linear mixed models (GLMM, for those cases where we set some of the factors as random) from the *R* package lme4 (Bates *et al.*, 2015). The effect of soil type and drought treatment over the course of the experiment on GWC, plant water potentials at predawn (Ψ_{pd}), midday (Ψ_{md}), the difference between them ($\Delta\Psi$) and the isotopic composition of the different water pools (soils, stems, roots and rocks) was tested with GLMs with interactions between all factors. In order to determine the most relevant factors explaining the variability in

isotopic offsets ($\Delta^{18}O$ and $\Delta^{2}H$, calculated as the difference between plant and soil water isotopic composition), we conducted a stepwise regression model. In the saturated model, we considered, θ_{rel}, soil type, g_s, Ψ_{pd} and Ψ_{md}. Based on the Akaike Information Criterion (AIC) (Akaike, 1974), we progressively removed those variables that were not significant, deciding to maintain this removal if the AIC decreased (better compromise between goodness of fit and model simplicity).

3. Results

3.1 Manipulation effects on soil water content and plant water use

Soil gravimetric water content (GWC) decreased over time ($P < 0.001$) in the drought treatment, while it was maintained in the control treatment (Fig. 2). Soil type had a significant effect on the drying rate ($P = 0.001$ for the soil type × time × treatment interaction), with fastest drying rates in the rocky sandy soil and slowest drying rates in the sandy clay loam (Fig. S2).

Predawn leaf water potential (Ψ_{pd}) also decreased over time in the drought treatment while it was maintained in control pots ($P < 0.001$, for the treatment effect, Fig. 2). The impact of the drought treatments on GWC was observed rapidly in the different soils, but differences in Ψ_{pd} ($P > 0.15$ for soil type and its interactions) started to decline only 20 days after the last watering event (Fig. S2). Similarly, plants in the drought treatment had more negative Ψ_{md} and smaller $\Delta\Psi$ than plants in the control treatment ($P = 0.04$ and 0.001, for Ψ_{md} and $\Delta\Psi$, respectively), but with no significant difference between soil types (Fig. S3). Plants in the control treatment had higher g_s than plants in the drought treatment ($P < 0.001$) (Fig. 2) and did not show any difference in stomatal conductance (g_s) between soil types (not shown). The deliberate reduction in VPD promoted by bagging the plants overnight prior to the first two sampling dates successfully increased g_s, but did not affect predawn water potentials (not shown).

Plant water content was not sensitive to the drought treatment. Both control and drought plants showed a progressive decrease in root and stem water content (relative to total weight) over the experiment, with no significant difference between treatments (Fig. 2). Roots always had significantly higher water content than stems. Overall, the drought treatment had a significant influence on the plant water status only for the last two sampling campaigns (i.e. when predawn water potential fell below -1MPa), coinciding with significantly lower leaf stomatal conductance

and predawn water potential despite similar root and stem water contents, compared to the control plants.

3.2 Manipulation effects on the isotopic composition of water pools

The isotopic composition of soil water was always equal to or more enriched (i.e. had higher $\delta^{18}O$ and $\delta^{2}H$) than irrigation water, even in the (regularly irrigated) control treatment (Figs. 3 and 4). This isotopic enrichment above irrigation water of soil water in the control treatment was stronger when the time between the last irrigation and the date of sampling was longer, and comparable to the enrichment in the drought treatment during the first three campaigns. In the drought treatment, and despite our attempt to prevent soil evaporation, the $\delta^{18}O$ of soil water increased over time, especially over the last two sampling campaigns (Fig. 3). In contrast, soil water $\delta^{2}H$ did not follow a progressive enrichment as the soil dried, as it is expected from soil evaporative enrichment theory (Barnes & Allison, 1983). These patterns were visible and reproducible amongst all soil types (Fig. S4).

Root and stem water $\delta^{18}O$ broadly reflected the $\delta^{18}O$ of the corresponding soil water (Fig. 3). In contrast, root and stem water $\delta^{2}H$ from the control treatment was always more depleted than soil water $\delta^{2}H$ ($P < 0.001$ and $P < 0.01$, Fig. 3). A similar pattern was also visible in the drought treatment for the first three sampling campaigns (i.e. until the drought treatment had a significant influence on the plant water status, see section 3.1). However, for the last two campaigns, root and stem water $\delta^{2}H$ started to increase and became more enriched than soil water $\delta^{2}H$ (Fig. 3). No significant difference was found between root and stem water $\delta^{2}H$.

Differences in the isotopic compositions of stem, root and soil water described above were not affected by soil type (Fig. S4). However, water extracted from limestone rocks was more enriched than soil water in response to drought in both $\delta^{18}O$ ($P < 0.05$) and $\delta^{2}H$ ($P < 0.001$) but this did not affect the isotopic composition of plant and soil water pools (Fig. S4).

3.3 Isotopic offsets between plant and soil water pools

Although soil, root and stem water $\delta^{18}O$ and $\delta^{2}H$ behaved differently upon drying, a strong correlation between $\delta^{18}O$ and $\delta^{2}H$ soil-plant offsets ($\Delta^{18}O$ and $\Delta^{2}H$), for both roots and stems was observed (Fig. 5). The slope of the orthogonal distance linear regression (that accounts for errors

on both axes) between $\Delta^{18}O$ and $\Delta^{2}H$ was 7.9 ±0.7 and 7.2 ±0.8 for soil-stem and soil-root offsets, respectively.

The $\delta^{2}H$ soil-stem water offset ($\Delta^{2}H$) was significantly different from zero ($P < 0.001$) for control plants, with a mean value of 10.6 ± 3.05‰, indicating that stem water was significantly more depleted than soil water (Figs. S5). In the drought treatment, $\Delta^{2}H$ shifted from positive to negative values over time ($P < 0.001$, Fig. S5), indicating that stem water became significantly more enriched in ^{2}H than the corresponding soil water. This shift occurred only when soil water content was below the permanent wilting point (Fig. S5), and when the drought treatment started to have significant effects on leaf stomatal conductance and predawn water potential (Fig. 2). The $\delta^{18}O$ soil-stem water offset ($\Delta^{18}O$) was not significantly different from zero in both treatments (Fig. S5a,c), although $\Delta^{18}O$ co-varied with $\Delta^{2}H$ (Fig. 4). Therefore, stem $\delta^{18}O$ reflected soil water $\delta^{18}O$. Because root and stem water did not differ significantly in their isotopic composition, soil-root isotopic offsets followed similar patterns as soil-stem $\Delta^{2}H$ and $\Delta^{18}O$ (Fig. S5b,d). The effect of θ_{rel} was significant and negative for $\Delta^{18}O$, but negligible for $\Delta^{2}H$ (Fig. 6). For both $\Delta^{18}O$ and $\Delta^{2}H$, we found positive effects of Ψ_{md} and $\Delta\Psi$ (Table 1). Leaf $\Delta\Psi$ was the variable that explained the largest part of the variance in $\Delta^{18}O$ and $\Delta^{2}H$. The larger the leaf $\Delta\Psi$, the larger the soil-stem isotopic offsets (Fig. 7 and Table 1). Finally, pots exposed to a low VPD treatment had significantly lower soil-stem $\Delta^{2}H$ than ambient VPD plants ($P < 0.05$), but not significantly different $\Delta^{18}O$ (Fig. S6). Plant water content, either in roots or stems, did not explain the isotopic differences between treatments.

4. Discussion

Our results from a controlled experiment with potted *F. sylvatica* saplings revealed that hydrogen isotope offsets between soil and plant water pools ($\Delta^{2}H$) are consistent over a range of soil types but highly dependent on plant water status. As long as soil water remained above the permanent wilting point, stem and root water were significantly more depleted in ^{2}H than their corresponding source water (Figs. 3 and S5), leading to a soil-stem isotopic offset in $\Delta^{2}H$ of a similar magnitude to those observed in the field for adult *F. sylvatica* and *Quercus robur* trees (Goldsmith *et al.*, 2018; Barbeta *et al.*, 2019) and a number of other species (Lin & Sternberg, 1993; Ellsworth & Williams, 2007; Brooks *et al.*, 2010; Zhao *et al.*, 2016; Evaristo *et al.*, 2017; Brum *et al.*, 2018; Oerter & Bowen, 2019). The reproducibility of this offset in potted and

399 irrigated *F. sylvatica* saplings demonstrates that soil-plant isotopic offset is not restricted to
400 halophytes (Lin & Sternberg, 1993; Ellsworth & Williams, 2007; Eley *et al.*, 2014; Redelstein *et*
401 *al.*, 2018) or xerophytes (Ellsworth & Williams, 2007; Zhao *et al.*, 2016) but is more general and
402 can occur as well in temperate forests. It further suggests that, in the field, soil-plant δ^2H offsets
403 cannot be solely attributed to a missing water source (Oerter & Bowen, 2019; Oerter *et al.*,
404 2019). Our results that the isotope offset can be cancelled or even reversed when predawn water
405 potential drops below - 1MPa in *F. sylvatica* may also explain why some field studies do not
406 observe such an offset, especially in semi-arid sites (e.g. Grossiord et al., 2016) or in temperate
407 sites during the dry season (e.g. Bariac *et al.*, 1990). The long-standing principle that there is no
408 isotopic fractionation within soil and stem water pools requires reconsideration, at least for δ^2H.
409 Meanwhile, oxygen isotope offsets ($\Delta^{18}O$) between soil and plant water were also present and
410 proportional to Δ^2H (Fig. 5), although not always significant (Fig. S5).

411 Vargas *et al.* (2017) performed a similar experiment on potted *Persea americana* plants and
412 found soil-stem isotopic offsets that were comparable to those reported here. Their soil-stem Δ^2H
413 and $\Delta^{18}O$ showed a linear relationship with a slope of 10.6±3.8, i.e., in the same range as the
414 ones reported here (7.9±0.7 for soil-stem offsets). However, because they explored a narrower
415 range of soil water availability, they did not detect the sign inversion in both $\Delta^{18}O$ and Δ^2H as
416 found here when Ψ_{pd} fell below -1 MPa (Fig. S5). Vargas et al. (2017) explained the observed
417 soil-stem isotopic offset by a putative isotope fractionation process during root water uptake (see
418 Introduction). However, our results from the control treatment do not support this hypothesis, as
419 theoretically, this would result in an enrichment of soil water whilst stem water would reflect
420 irrigation water (Fig. 1A, see the theoretical framework in Supplementary Information). In
421 contrast, we found a strong depletion of stem water δ^2H compared to irrigation water in the
422 control treatments that cannot be explained by root discrimination and/or soil evaporation (see
423 Supplementary Information). A more likely explanation for the isotopic depletion of bulk stem
424 water compared to soil water in our experiment (and that of Vargas *et al.*) is that storage water in
425 the xylem tissue is depleted compared to vessel water (i.e. sap) (Fig. 1B).

426 Such isotopic offsets between bulk stem water and vessel (sap) water have been reported in
427 woody plants (Zhao *et al.*, 2016). In addition, large isotopic differences between leaf water pools
428 from the multiple epidermis (storage tissues) (White *et al.*, 1985) and the spongy parenchyma

(photosynthetic tissues) of the CAM plant *Peperomia congesta* (HBK) have also been documented (Yakir *et al.*, 1994). The isotopic difference between storage and photosynthetic tissues was comparable to the isotopic offsets reported here between soil and stem water (i.e. >10‰). Interestingly this isotopic difference was maintained only under turgid conditions and vanished under water limitations (Yakir *et al*., 1994). This is coherent with our findings that the isotopic offsets between soil and stem water vanishes around the permanent wilting point (Fig. 6). However this would imply that, under low transpiration, the mixing of the storage and vessel water in the stem becomes more pronounced, resulting in a lower fractionation between the two water pools (ε_x in Fig. 1B). Such a reduction of ε_x under water limitations would need to be tested using techniques that allow isotopic determination of vessel and stem tissue water separately. However, a reduction of ε_x cannot explain why stem water becomes more enriched than soil water below the permanent wilting point (Fig. 6). A plausible explanation for this pattern is that, when water is limited, stem evaporation (E_x) enriches stem water above the values of soil water, because the transpiration stream cannot replenish the stem tissue at a fast enough rate (Martin-Gomez *et al*., 2017).

It remains to be explained why, in the drought treatment, soil water $\delta^{18}O$ increases continuously while its $\delta^{2}H$ counterpart remains constant or even decreases once permanent wilting point is reached (Fig. 3). A very similar pattern had already been observed on wheat and sunflower, and had been interpreted as a possible effect of plant organic matter decomposition (Allison *et al.*, 1984). Vargas *et al*. (2017) rejected this idea on the basis that, in their experiment, potted cut stems (that had decaying roots and no transpiring canopy) did not produce any depletion in soil water $\delta^{2}H$. However, soil water in pots with live plants was not depleted either in their experiment and, as mentioned above, they did not explore the full range of water potentials that were explored in this study or in Allison *et al*. (1983). Our data demonstrated that only once permanent wilting point had been reached and predawn water potential dropped below -1 MPa, did soil water $\delta^{18}O$ and $\delta^{2}H$ start to exhibit clear opposite trends. Thus, we hypothesise that Vargas *et al*. did not observe the same trends as here because the drought treatment they applied was too mild. In addition, we propose an alternative explanation to that of Allison *et al*. (1983) and suggest that this pattern in soil water isotopes under dry conditions results from surface isotope effects. Indeed, as soil dries adsorbed water becomes an increasingly larger fraction (f_a) of total soil water (Tuller & Or, 2005; Chen *et al.*, 2016; Lu, 2016). In the two last sampling

460 campaigns of our experiment, soil GWC was below 0.1 $g.g^{-1}$ (11% VWC) in the drought
461 treatment (Fig. 2). According to Lu (2016), adsorbed water can range from 1.7% VWC in sandy
462 soils to 12.8% VWC in silty clay soils. It is thus reasonable to assume that the isotopic
463 fractionation associated with adsorbed water can dominate the isotopic composition of dry soils.
464 Meanwhile, under sustained drought, the remaining bulk soil water would still become
465 progressively enriched because of soil evaporation (E_s). Depending on the balance between the
466 enrichment caused by evaporation and the depletion caused by the higher fraction of adsorbed
467 water, the isotopic composition of bulk soil water could show different trends during drying
468 periods, either positive or negative. Because soil evaporative enrichment creates a relatively
469 stronger enrichment in ^{18}O than in ^{2}H (i.e. the slope of the evaporation line in the dual isotope
470 space is lower than the slope of the meteoric water line) and surface isotope effects are much
471 stronger for ^{2}H than for ^{18}O (Chen *et al.*, 2016; Lin *et al.*, 2018), it is plausible that soil water
472 $\delta^{18}O$ enriches while soil water $\delta^{2}H$ becomes depleted, at least when the soil water balance is
473 dominated by root water uptake. In the field, this opposing trend between soil water $\delta^{18}O$ and
474 $\delta^{2}H$ may be harder to observe as capillary rise may compensate water losses, minimising the
475 influence of adsorbed water, and the depletion of soil water above the evaporation front may be
476 dominated by the back diffusion of (depleted) atmospheric vapour into the soil (Barnes &
477 Allison, 1983).

478 In conclusion, we propose the following explanation for the dynamics of soil-plant isotopic
479 offsets reported here and in other studies. This is the most plausible explanation, but it is still
480 untested in a qualitative sense. Plants take up mobile and capillary soil water during
481 transpiration. In wet conditions (control treatment), this soil water pool constitutes a large
482 fraction of bulk soil water with an isotopic composition (δ_m) close to that of irrigation water.
483 However, bulk stem water is depleted compared to mobile and capillary soil water (Zhao *et al.*,
484 2016) because it comprises a mix of vessel water that reflects mobile/capillary soil water, with
485 storage water that is depleted compared to vessel water (Fig. 8A). The origin of this depletion of
486 storage water in the stem is unknown, but could be related to surface processes on plant organic
487 surfaces (Chen *et al.*, 2016). In contrast, during dry conditions (drought treatment), adsorbed
488 water represents an increasingly larger fraction of bulk soil water, creating a significant depletion
489 of bulk soil water compared to mobile/capillary water, and thus compared to vessel water in a
490 transpiring plant. Bulk stem water remains depleted compared to vessel water but, as plant

transpiration becomes strongly reduced under prolonged drought, stem evaporation (E_x) increasingly enriches bulk stem water above the composition of soil mobile/capillary water (δ_m) (Fig. 8B). Our findings that the isotopic offsets between soil and stem water increase with plant transpiration proxies such as the diurnal amplitude of stem water potential $\Delta\Psi$ (Fig. 7) or stomatal conductance (Fig. S7) indicate that soil-stem isotopic offsets also reflect the competition between transpiration and stem evaporation (Martín-Gómez *et al.*, 2017) and the matric potential of soil and plant water pools (Gaj & McDonnell, 2019).

Acknowledgements

Many thanks to Steven Wohl, Nicolas Devert, Céline Gire, Lionel Jordan-Meille and the staff at Bordeaux Science Agro for technical support, as well as Nicolas Cornette, Yann Cochet and Kenza Bakouri for assistance in the glasshouse. This study received funding from the EC2CO/BIOHEFECT program (CNRS, France), the French national research agency (projects Hydrobeech, Climbeech and Micromic within the Cluster of Excellence COTE with grant agreement ANR-10-LABX-45; project ORCA with grant agreement ANR-13-BS06-0005-01), the European Research Council (ERC) under the EU Seventh Framework Program (FP7/2007-2013, with grant agreement no. 338264, awarded to L.W) and the Aquitaine Region (project Athene with grant agreement 2016-1R20301-00007218). A.B. also acknowledges an IdEx Bordeaux postdoctoral fellowship from the Université de Bordeaux (contract no. 22001162).

Author contributions

A.B., T.E.G. and J.O. designed the study; T.E.G., L.C., A.B. and C.D. grew plants, applied irrigation treatments and measured soil and plant parameters; A.B., B.F., S.P.J. and J.O. performed stable isotope analyses; A.B. and J.O wrote the manuscript with contributions from all authors.

References

Akaike H. **1974**. A New Look at the Statistical Model Identification. *IEEE Transactions on Automatic Control* **19**: 716–723.

Allison GB, Barnes CJ, Hugues MW, Leaney FWJ. **1984**. Effect of Climate and Vegetation on Oxygen-18 and Deuterium Profiles in Soils. *Isotope hydrology, 1983 : proceedings of an International Symposium on Isotope Hydrology in Water Resources Development*: 105–123.

Barbeta A, Jones SP, Clavé L, Wingate L, Gimeno TE, Fréjaville B, Wohl S, Ogée J. **2019**. Unexplained hydrogen isotope offsets complicate the identification and quantification of tree water sources in a riparian forest. *Hydrology and Earth System Sciences* **23**: 1–31.

Barbeta A, Mejía-Chang M, Ogaya R, Voltas J, Dawson TE, Peñuelas J. **2015**. The combined effects of a long-term experimental drought and an extreme drought on the use of plant-water sources in a Mediterranean forest. *Global Change Biology* **21**: 1213–1225.

Barbeta A, Peñuelas J. **2017**. Relative contribution of groundwater to plant transpiration estimated with stable isotopes. *Scientific Reports* **7**: 1–10.

Bariac T, Jusserand C, Mariotti A. **1990**. Evolution de la composition isotopique de l'eau (18O) dans le continuum sol-plante-atmosphere. *Catena* **54**: 413–424.

Barnes CJ, Allison GB. **1983**. The distribution of deuterium and 18O in dry soils. *Journal of Hydrology* **60**: 141–156.

Bates D, Mächler M, Bolker B, Walker S. **2015**. Fitting Linear Mixed-Effects Models using lme4. *Journal of Statistical Software* **67**.

Bertrand G, Masini J, Goldscheider N, Meeks J, Lavastre V, Celle-Jeanton H, Gobat JM, Hunkeler D. **2014**. Determination of spatiotemporal variability of tree water uptake using stable isotopes (δ18O, δ2H) in an alluvial system supplied by a high-altitude watershed, Pfyn forest, Switzerland. *Ecohydrology* **7**: 319–333.

Bowling DR, Schulze ES, Hall SJ. **2017**. Revisiting streamside trees that do not use stream water: can the two water worlds hypothesis and snowpack isotopic effects explain a missing water source? *Ecohydrology* **10**: 1–12.

Brian Leen J, Berman ESF, Liebson L, Gupta M. **2012**. Spectral contaminant identifier for off-axis integrated cavity output spectroscopy measurements of liquid water isotopes. *Review of Scientific Instruments* **83**.

Brooks JR, Barnard HR, Coulombe R, McDonnell JJ, Renée Brooks J, Barnard HR, Coulombe R, McDonnell JJ. **2010**. Ecohydrologic separation of water between trees and streams in a Mediterranean climate. *Nature Geoscience* **3**: 100–104.

Brum M, Vadeboncoeur MA, Ivanov V, Asbjornsen H, Saleska S, Alves LF, Penha D, Dias JD, Aragão LEOC, Barros F, *et al.* 2018. Hydrological niche segregation defines forest structure and drought tolerance strategies in a seasonal Amazon forest. *Journal of Ecology*: 318–333.

Chen G, Auerswald K, Schnyder H. **2016**. 2H and 18O depletion of water close to organic surfaces. *Biogeosciences* **13**: 3175–3186.

Dawson TE, Ehleringer JR. **1991**. Streamside trees that do not use stream water. *Nature* **350**: 335–337.

De Deurwaerder H, Hervé-Fernández P, Stahl C, Burban B, Petronelli P, Hoffman B, Bonal D, Boeckx P, Verbeeck H. **2018**. Liana and tree below-ground water competition—evidence for water resource partitioning during the dry season. *Tree Physiology*: 1–13.

Eley Y, Dawson L, Black S, Andrews J, Pedentchouk N. **2014**. Understanding 2 H / 1 H systematics of leaf wax n -alkanes in coastal plants at Stiffkey saltmarsh , Norfolk , UK. *Geochimica et Cosmochimica Acta* **128**: 13–28.

Ellsworth PZ, Williams DG. **2007**. Hydrogen isotope fractionation during water uptake by woody xerophytes. *Plant and Soil* **291**: 93–107.

Evaristo J, McDonnell JJ, Clemens J. **2017**. Plant source water apportionment using stable isotopes: A comparison of simple linear, two-compartment mixing model approaches. *Hydrological Processes* **31**: 3750–3758.

Gaj M, McDonnell JJ. **2019**. Possible soil tension controls on the isotopic equilibrium fractionation factor for evaporation from soil. *Hydrological Processes* **33**: 1629–1634.

Geris J, Tetzlaff D, McDonnell JJ, Soulsby C. **2017**. Spatial and temporal patterns of soil water storage and vegetation water use in humid northern catchments. *Science of the Total Environment* **595**: 486–493.

Goldsmith GR, Allen ST, Braun S, Engbersen N, Romero González-Quijano C, Kirchner JW, Siegwolf RTW. **2018**. Spatial variation in throughfall, soil, and plant water isotopes in a temperate forest. *Ecohydrology*: e2059.

Jasechko S, Sharp ZD, Gibson JJ, Birks SJ, Yi Y, Fawcett PJ. **2013**. Terrestrial water fluxes dominated by transpiration. *Nature* **496**: 347–350.

Jones SP, Ogée J, Sauze J, Wohl S, Saavedra N, Fernández-Prado N, Maire J, Launois T, Bosc A, Wingate L. **2017**. Non-destructive estimates of soil carbonic anhydrase activity and associated soil water oxygen isotope composition. *Hydrology and Earth System Sciences* **21**: 6363–6377.

Lin Y, Horita J. **2016**. An experimental study on isotope fractionation in a mesoporous silica-water system with implications for vadose-zone hydrology. *Geochimica et Cosmochimica Acta* **184**: 257–271.

Lin Y, Horita J, Abe O. **2018**. Adsorption isotope effects of water on mesoporous silica and alumina with implications for the land-vegetation-atmosphere system. *Geochimica et Cosmochimica Acta* **223**: 520–536.

Lin G, Sternberg L da SL. **1993**. Hydrogen isotopic fractionation by plant roots during water uptake in coastal wetland plants. In: Ehleringer J, Hall A, Farquhar G, eds. Stable isotopes and plant carbon-water relations. New York: Academic Press Inc., 497–510.

Lu N. **2016**. Generalized soil water retention equation for adsorption and capillarity. *Journal of Geotechnical and Geoenvironmental Engineering* **142**.

Mahindawansha A, Orlowski N, Kraft P, Rothfuss Y, Racela H, Breuer L. **2018**. Quantification of plant water uptake by water stable isotopes in rice paddy systems. *Plant and Soil* **429**: 281–302.

Martín-Gómez P, Barbeta A, Voltas J, Peñuelas J, Dennis K, Palacio S, Dawson TE, Ferrio JP. **2015**. Isotope-ratio infrared spectroscopy: A reliable tool for the investigation of plant-water

sources? *New Phytologist* **1**.

Martín-Gómez P, Serrano L, Ferrio JP. **2017**. Short-term dynamics of evaporative enrichment of xylem water in woody stems: Implications for ecohydrology. *Tree Physiology* **37**: 511–522.

Millar C, Pratt D, Schneider D, McDonnell JJ. **2015**. A Comparison of Extraction Systems for Plant Water Stable Isotope Analysis. *Rapid Communications in Mass Spectometry*: 1–4.

Moreno-Gutiérrez C, Dawson TE, Nicolás E, Querejeta JI. **2012**. Isotopes reveal contrasting water use strategies among coexisting plant species in a Mediterranean ecosystem. *The New phytologist* **196**: 489–96.

Munksgaard NC, Cheesman AW, Wurster CM, Cernusak LA, Bird MI. **2014**. Microwave extraction-isotope ratio infrared spectroscopy (ME-IRIS): A novel technique for rapid extraction and in-line analysis of δ18O and δ2H values of water in plants, soils and insects. *Rapid Communications in Mass Spectrometry* **28**: 2151–2161.

Newberry SL, Nelson DB, Kahmen A. **2017**. Cryogenic vacuum artifacts do not affect plant water-uptake studies using stable isotope analysis. *Ecohydrology* **10**.

Oerter EJ, Bowen GJ. **2019**. Spatio-temporal heterogeneity in soil water stable isotopic composition and its ecohydrologic implications in semiarid ecosystems. *Hydrological Processes* **33**: 1724–1738.

Oerter E, Finstad K, Schaefer J, Goldsmith GR, Dawson T, Amundson R. **2014**. Oxygen isotope fractionation effects in soil water via interaction with cations (Mg, Ca, K, Na) adsorbed to phyllosilicate clay minerals. *Journal of Hydrology* **515**: 1–9.

Oerter EJ, Siebert G, Bowling DR, Bowen G. **2019**. Soil water vapour isotopes identify missing water source for streamside trees. *Ecohydrology* **12**: 0–1.

Orlowski N, Breuer L, Angeli N, Boeckx P, Brumbt C, Cook CS, Dubbert M, Dyckmans J, Gallagher B, Gralher B, *et al.* 2018. Inter-laboratory comparison of cryogenic water extraction systems for stable isotope analysis of soil water. *Hydrology and Earth System Sciences* **22**: 3619–3637.

Orlowski N, Frede H-G, Brüggemann N, Breuer L. **2013**. Validation and application of a

cryogenic vacuum extraction system for soil and plant water extraction for isotope analysis. *Journal of Sensors and Sensor Systems* **2**: 179–193.

Penna D, Hopp L, Scandellari F, Allen ST, Benettin P, Beyer M, Geris J, Klaus J, Marshall JD, Schwendenmann L, *et al.* 2018. Ideas and perspectives: Tracing terrestrial ecosystem water fluxes using hydrogen and oxygen stable isotopes - Challenges and opportunities from an interdisciplinary perspective. *Biogeosciences* **15**: 6399–6415.

Poca M, Coomans O, Urcelay C, Zeballos SR, Bodé S, Boeckx P. **2019**. Isotope fractionation during root water uptake by Acacia caven is enhanced by arbuscular mycorrhizas. *Plant and Soil* **441**: 485–497.

R Core Team. **2019**. R: A Language and Environment for Statistical Computing.

Raulerson SA. **2018**. Toward a Diffusive , Non-Destructive Approach to Measuring Stable Isotopes of Water within Tree Stems.

Redelstein R, Coners H, Knohl A, Leuschner C. **2018**. Water sources of plant uptake along a salt marsh flooding gradient. *Oecologia* **188**: 607–622.

Schultz NM, Griffis TJ, Lee X, Baker JM. **2011**. Identification and correction of spectral contamination in 2H/ 1H and 18O/ 16O measured in leaf, stem, and soil water. *Rapid Communications in Mass Spectrometry* **25**: 3360–3368.

Stumpp C, Brüggemann N, Wingate L. **2018**. Stable isotope approaches in vadose zone research. *Vadose Zone Journal* **17**.

Thorburn PJ, Walker GR, Brunel J -P. **1993**. Extraction of water from Eucalyptus trees for analysis of deuterium and oxygen-18: laboratory and field techniques. *Plant, Cell & Environment* **16**: 269–277.

Tuller M, Or D. **2005**. Water films and scaling of soil characteristic curves at low water contents. *Water Resources Research* **41**: 1–6.

Vargas AI, Schaffer B, Yuhong L, Sternberg L da SL. **2017**. Testing plant use of mobile vs immobile soil water sources using stable isotope experiments. *New Phytologist* **215**: 582–594.

Walker CD, Richardson SB. **1991**. The use of stable isotopes of water in characterising the

source of water in vegetation. *Chemical Geology* **94**: 145–158.

Walker GR, Woods PH, Allison GB. **1994**. Interlaboratory comparison of methods to determine the stable isotope composition of soil water. *Chemical Geology* **111**: 297–306.

Wang J, Fu B, Lu N, Zhang L. **2017**. Seasonal variation in water uptake patterns of three plant species based on stable isotopes in the semi-arid Loess Plateau. *Science of the Total Environment* **609**: 27–37.

Washburn EW, Smith ER. **1934**. The isotopic fractionation of water by physiological processes. *Science* **79**: 188–189.

Wassenaar LI, Hendry MJ, Chostner VL, Lis GP. **2008**. High resolution pore water δ2H and δ18O measurements by H2O(liquid)-H2O (vapor) equilibration laser spectroscopy. *Environmental Science and Technology* **42**: 9262–9267.

White J, Cook E, Lawrence J, Broecker W. **1985**. The D/H Ratios of Sap in Trees - Implications for Water Sources and Tree-Ring D/H Ratios. *Geochimica Et Cosmochimica Acta* **49**: 237–246.

Yakir D, Ting I, DeNiro M. **1994**. Natural Abundance 2H/1H Ratios of Water Storage in Leaves of Peperomia Congesta HBK during Water Stress. *Journal of Plant Physiology* **144**: 607–612.

Zhao L, Wang L, Cernusak LA, Liu X, Xiao H, Zhou M, Zhang S. **2016**. Significant Difference in Hydrogen Isotope Composition Between Xylem and Tissue Water in Populus Euphratica. *Plant Cell and Environment* **39**: 1848–1857.

Zimmermann U, Ehhalt D, Münnich KO. **1967**. Soil-water movement and evapotranspiration: changes in the isotopic composition of the water. In: Isotopes in hydrology: Proceedings of a symposium. Vienna: International Atomic Energy Agency, 576–585.

679

680

681

682 **Table 1.** Output of the stepwise regression models for the soil-plant isotopic offsets. Effects
683 include VWC relative to VWC at the permanent wilting point (θ_{rel}), leaf midday water potential
684 (Ψ_{md}) and the daily difference between predawn and midday water potential ($\Delta\Psi$). 'Std. Error'
685 corresponds to the standard error of the mean.

686

		Estimate	Std. Error	*t*-value	*P*-value	R^2
$\Delta^{18}O$	Intercept	0.12	0.43	0.76	0.79	
	θ_{rel}	-2.59	1.01	-2.56	0.01	0.08
	Ψ_{md}	0.81	0.19	4.32	<0.0001	0.19
	$\Delta\Psi$	1.57	0.28	5.60	<0.0001	0.24
	Model R^2					0.36
$\Delta^{2}H$	Intercept	6.36	2.27	2.81	<0.01	
	θ_{rel}	3.87	5.30	0.73	0.47	0.007
	Ψ_{md}	5.91	0.98	6.05	<0.0001	0.32
	$\Delta\Psi$	9.6	1.47	6.55	<0.0001	0.36
	Model R^2					0.55

687

688

689 **Figure captions**

690 **Figure 1. Illustration of the expected isotopic composition of bulk soil (δ_{soil}) and stem (δ_{stem})**
691 **water when irrigation (*P*, with a constant isotopic composition δ_P) continuously**
692 **compensates root water uptake (*U*) and transpiration (*T*), and evaporation losses are**
693 **negligible (i.e. control treatments).** (a) scenario when root water uptake fractionates water
694 isotopes (fractionation factor ε_U) and (b) scenario when adsorbed water in the soil (fraction f_a)
695 and the stem's storage tissue water (fraction f_x) are depleted with respect to mobile and capillary
696 water in the soil (fractionation ε_a) and the xylem's vessel water(fractionation ε_x).

697 **Figure 2. Time course of soil and plant water status over the experiment.** Mean soil
698 gravimetric water content (GWC), leaf predawn water potential (Ψ_{pd}), plant water content (roots
699 and stems) and stomatal conductance (g_s) over the course of the experiment in control (left
700 panels) and drought (right panels) treatments. Error bars are the standard error of the mean
701 (N = 30 and 15, for soil GWC and 15 and 9 for Ψ_{pd}, plant GWC and g_s for drought and control,
702 respectively).

703 **Figure 3. Time course of soil and plant water isotopic composition over the experiment.**
704 Mean δ^2H and $\delta^{18}O$ of soil, stem and root water over the course of the experiment in control (left
705 panels) and drought (right panels) treatments. Error bars are the standard error of the mean (N =
706 15 and 9, for drought and control, respectively) and can be masked by the symbol when too
707 small. The solid teal line corresponds to the mean of the isotopic composition of the irrigation
708 water and the dashed lines its standard error. Vertical arrows in the top panels indicate irrigation
709 times. On right panels, the vertical dashed line indicates the approximate time when the drought
710 treatment started to have significant effects on plant water status (Fig. 1).

711 **Figure 4. Dual isotope representation ($\delta^{12}H$ and $\delta^{18}O$) of soil, stem and root water.** (a)
712 Control treatment. (b) Drought treatment. Blue triangles indicate the isotopic composition of
713 irrigation water during the experiment and the dotted line represents the local meteoric water
714 line.

715 **Figure 5. Correlations between soil-plant $\delta^{18}O$ and δ^2H offsets.** (a) soil-stem offsets. (b)
716 soil)root offsets.

Figure 6. Effect of soil moisture on water isotopic compositions. Relationships between θ_{rel} (soil VWC relative to VWC at the permanent wilting point) and soil water δ^2H and $\delta^{18}O$ (left panels), stem water δ^2H and $\delta^{18}O$ (middle panels) and the soil-stem isotopic offsets $\Delta^{18}O$ and Δ^2H (right panels). Data were averaged by sampling date and irrigation and VPD treatments. Error bars are standard errors of the mean, and the dashed line indicates the isotopic composition of irrigation water (left and middle panels) or the zero (right panels).

Figure 7. Effect of plant ΔΨ on water isotopic compositions. Relationships between plant $\Delta\Psi$ (daily difference between Ψ_{pd} and Ψ_{md}) and soil water δ^2H and $\delta^{18}O$ (left panels), stem water δ^2H and $\delta^{18}O$ (middle panels) and soil-stem isotopic offsets $\Delta^{18}O$ and Δ^2H (right panels). Data were averaged by sampling date, and irrigation and VPD treatments. Error bars are standard errors of the mean, and the dashed line indicates the isotopic composition of irrigation water (left and middle panels) or the zero (right panels).

Figure 8. Illustration of the proposed effects on the isotopic composition (δ) of bulk soil (δ_{soil}) and stem (δ_{stem}) water in the present experiment, where soil (E_{soil}) and stem (E_{stem}) evaporation are not fully suppressed. (a) Control treatment with regular irrigation (*P* with constant isotopic composition, δ_P) compensating water losses through E_{soil} and root water uptake (*U,* further lost via transpiration *T* and E_{stem}). Here, the isotopic composition of soil mobile and capillary water (δ_m) and water inside the xylem vessels are expected to reflect δ_P with a possible enrichment due to soil evaporation occurring between irrigations events ($\geq\delta_P$), while soil capillary water (fraction f_a) and stem storage tissue water (fraction f_x) are depleted with respect to mobile soil water (fractionation ε_a) and to water inside the xylem conduits (fractionation ε_x). **(b)** Drought treatment with water losses via *T*, E_{soil} and E_{stem} not being compensated with *P*. Here, δ_m becomes progressively more enriched (due to soil evaporative enrichment) while the fraction of soil capillary water (f_a) increases. Resulting δ_{soil} either becomes more enriched (following δ_m) or more depleted (following f_a), depending on the balance between the two processes. Meanwhile, δ_{stem} becomes progressively more enriched, following δ_m because f_x varies proportionally less than f_a along the experiment (Fig. 2).

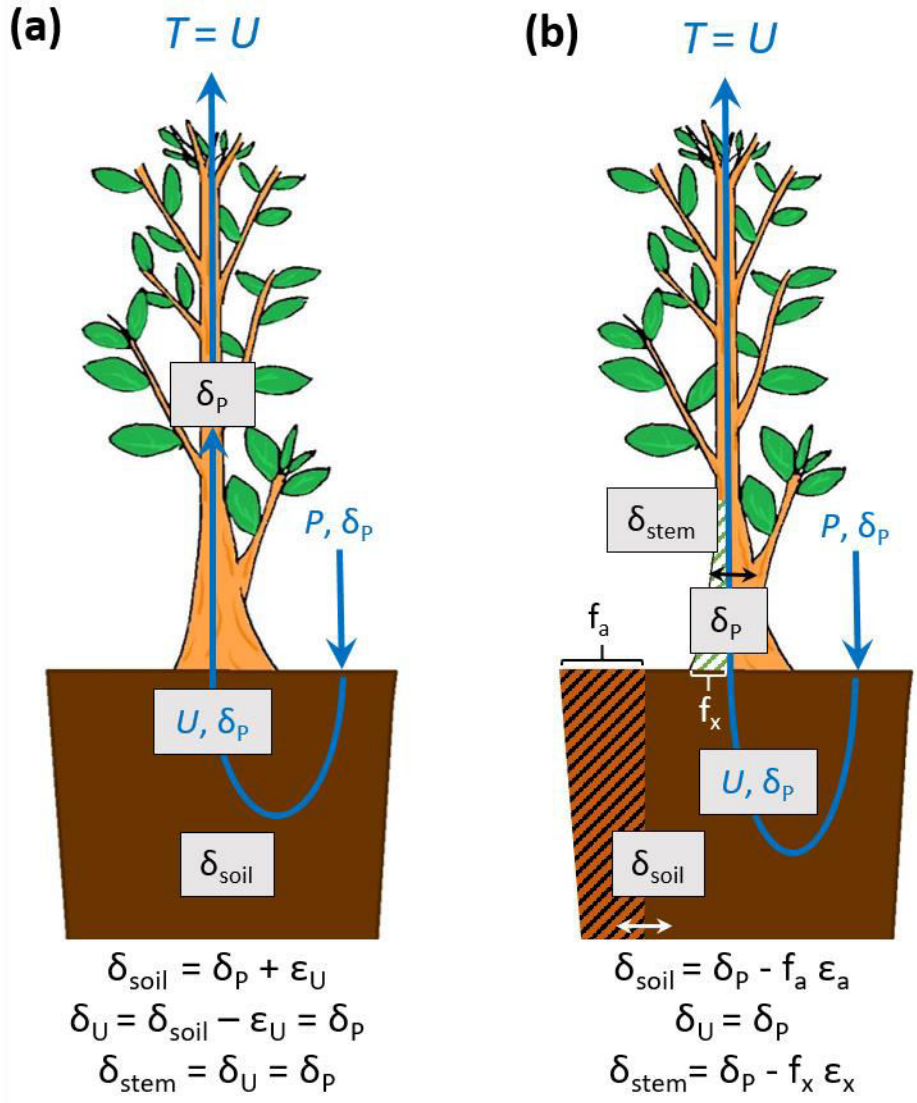

747

748

749

750

751

752

753

754

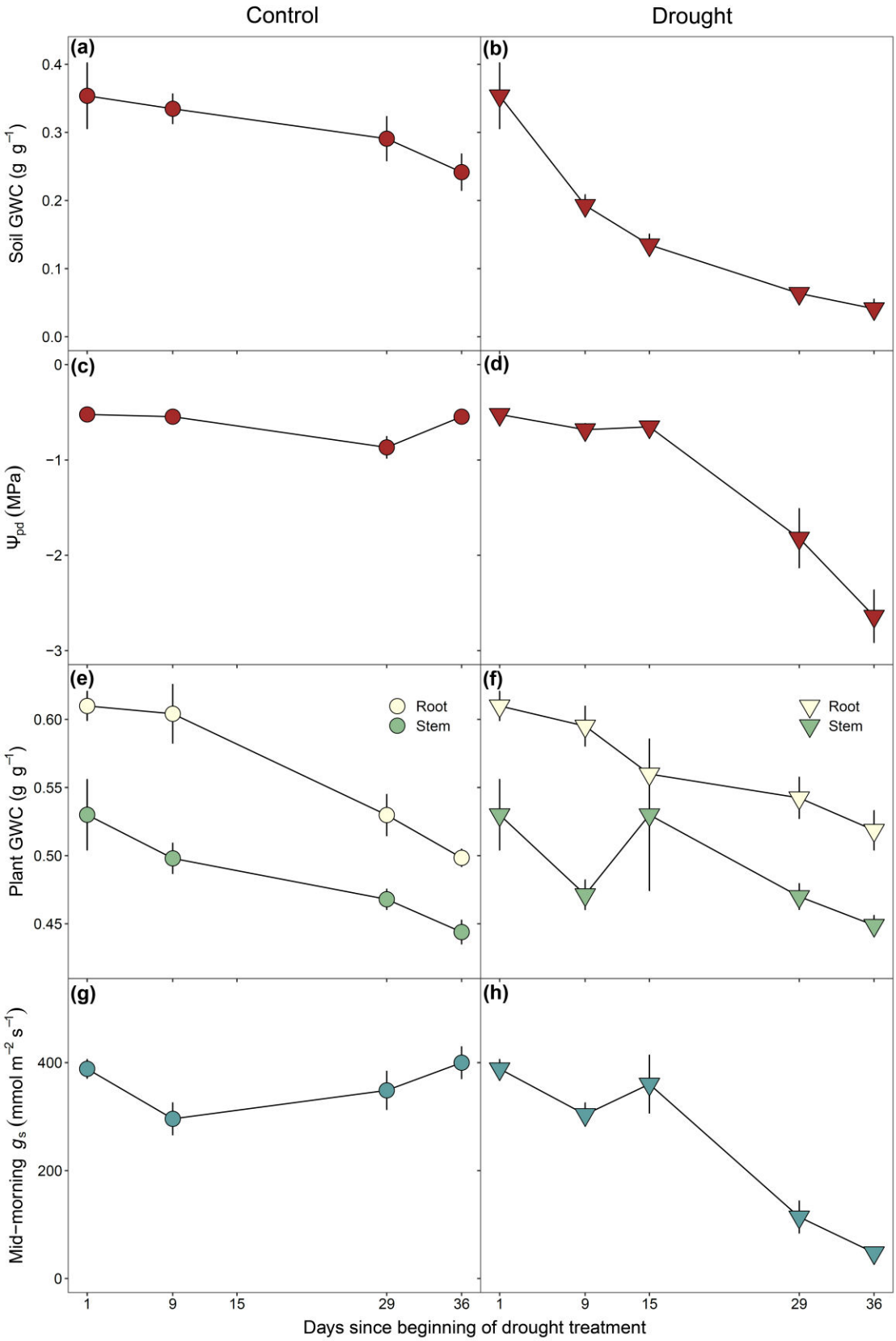
Control
Drought
(a)
(b)
(c)
(d)
(e)
(f)
(g)
(h)
Soil GWC (g g−1)
Ψpd (MPa)
Plant GWC (g g−1)
Mid−morning gs (mmol m−2 s−1)
Root
Stem
Days since beginning of drought treatment

755

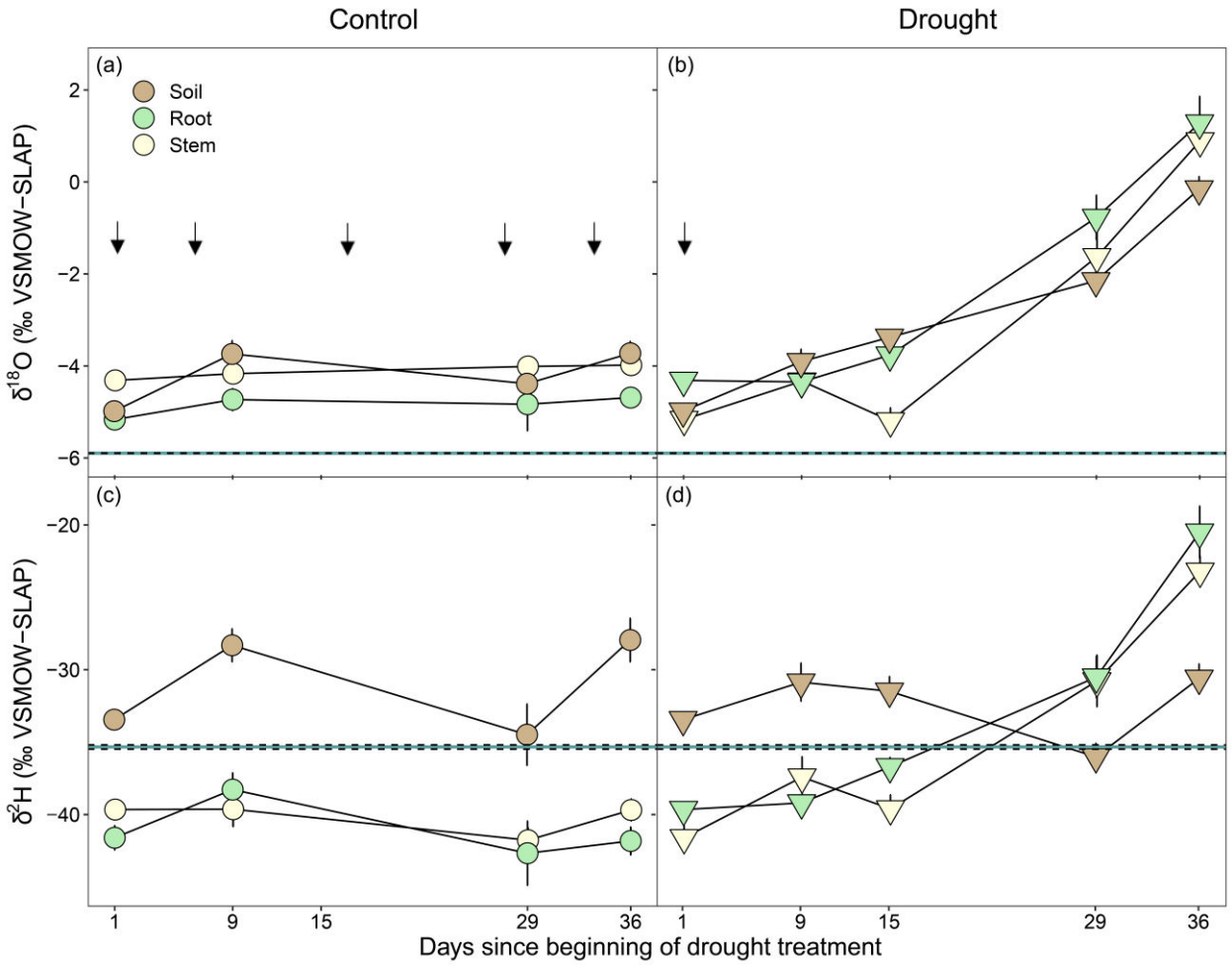
Control
Drought
(a)
(b)
(c)
(d)
Soil
Root
Stem
δ18O (‰ VSMOW−SLAP)
δ2H (‰ VSMOW−SLAP)
2
0
−2
−4
−6
−20
−30
−40
1
9
15
29
36
Days since beginning of drought treatment

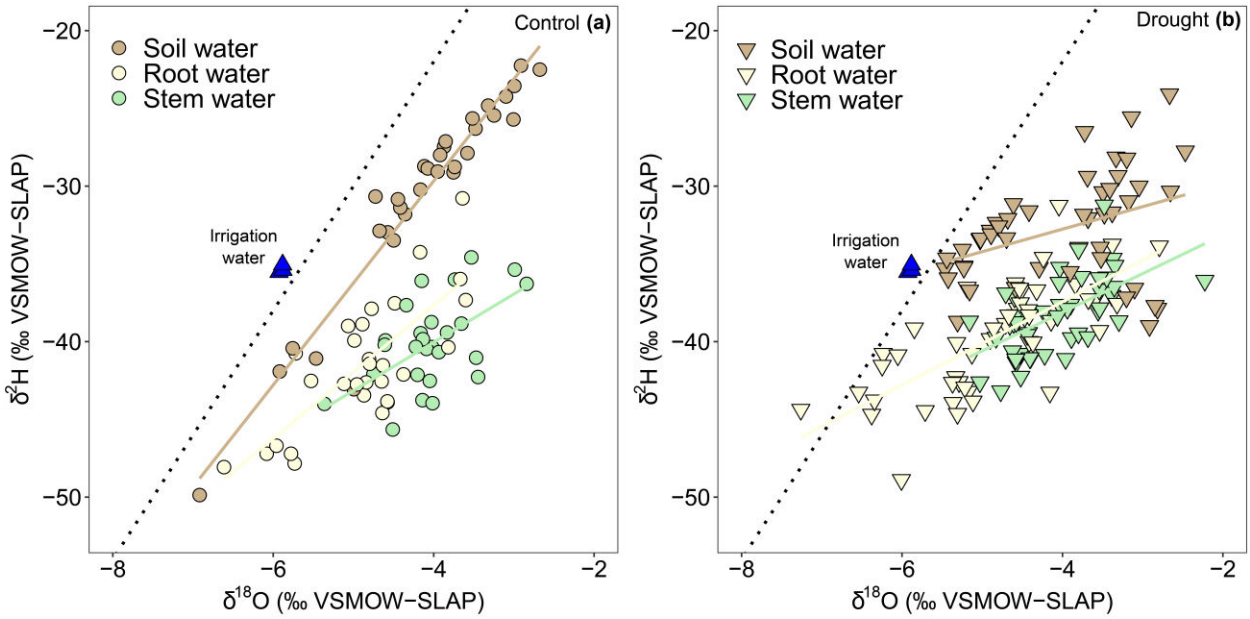
Control (a)
Soil water
Root water
Stem water
Irrigation water
δ2H (‰ VSMOW−SLAP)
δ18O (‰ VSMOW−SLAP)
−20
−30
−40
−50
−8
−6
−4
−2
Drought (b)
Soil water
Root water
Stem water
Irrigation water
δ2H (‰ VSMOW−SLAP)
δ18O (‰ VSMOW−SLAP)

768

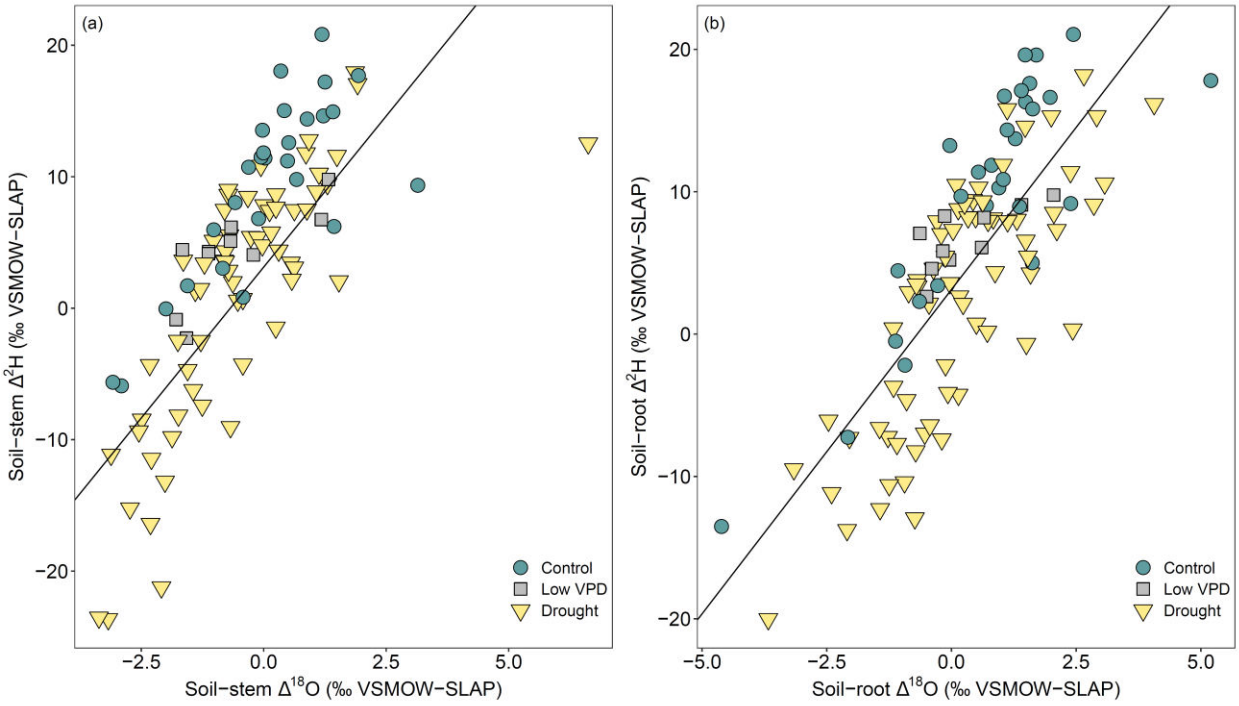
(a)
(b)
Soil−stem Δ2H (‰ VSMOW−SLAP)
Soil−stem Δ18O (‰ VSMOW−SLAP)
Soil−root Δ2H (‰ VSMOW−SLAP)
Soil−root Δ18O (‰ VSMOW−SLAP)
Control
Low VPD
Drought
20
10
0
−10
−20
−2.5
0.0
2.5
5.0
−5.0

769

770

771

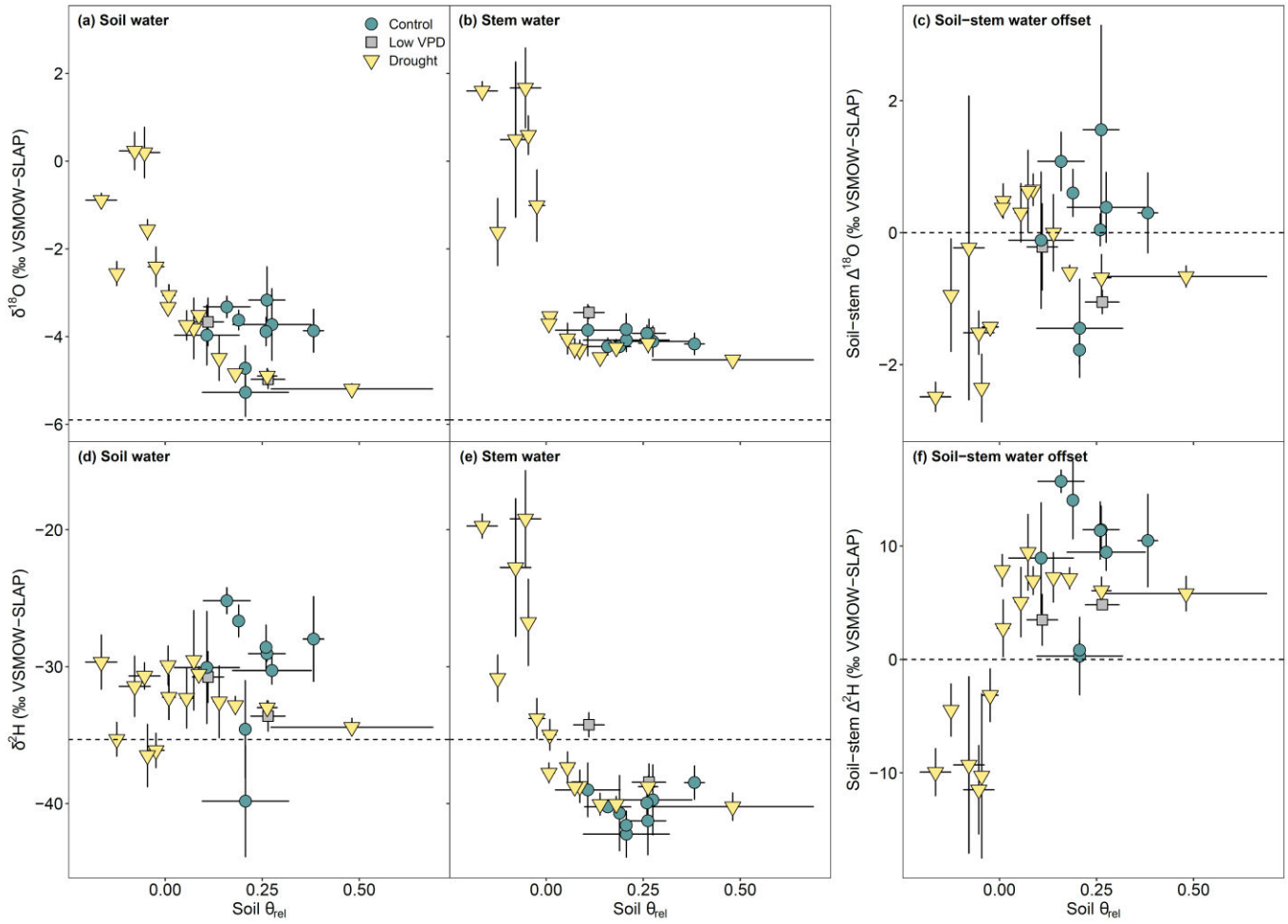
(a) Soil water
(b) Stem water
(c) Soil−stem water offset
(d) Soil water
(e) Stem water
(f) Soil−stem water offset
Control
Low VPD
Drought
δ18O (‰ VSMOW−SLAP)
δ2H (‰ VSMOW−SLAP)
Soil−stem Δ18O (‰ VSMOW−SLAP)
Soil−stem Δ2H (‰ VSMOW−SLAP)
Soil θrel
2
0
−2
−4
−6
−20
−30
−40
10
−10
0.00
0.25
0.50

772

773

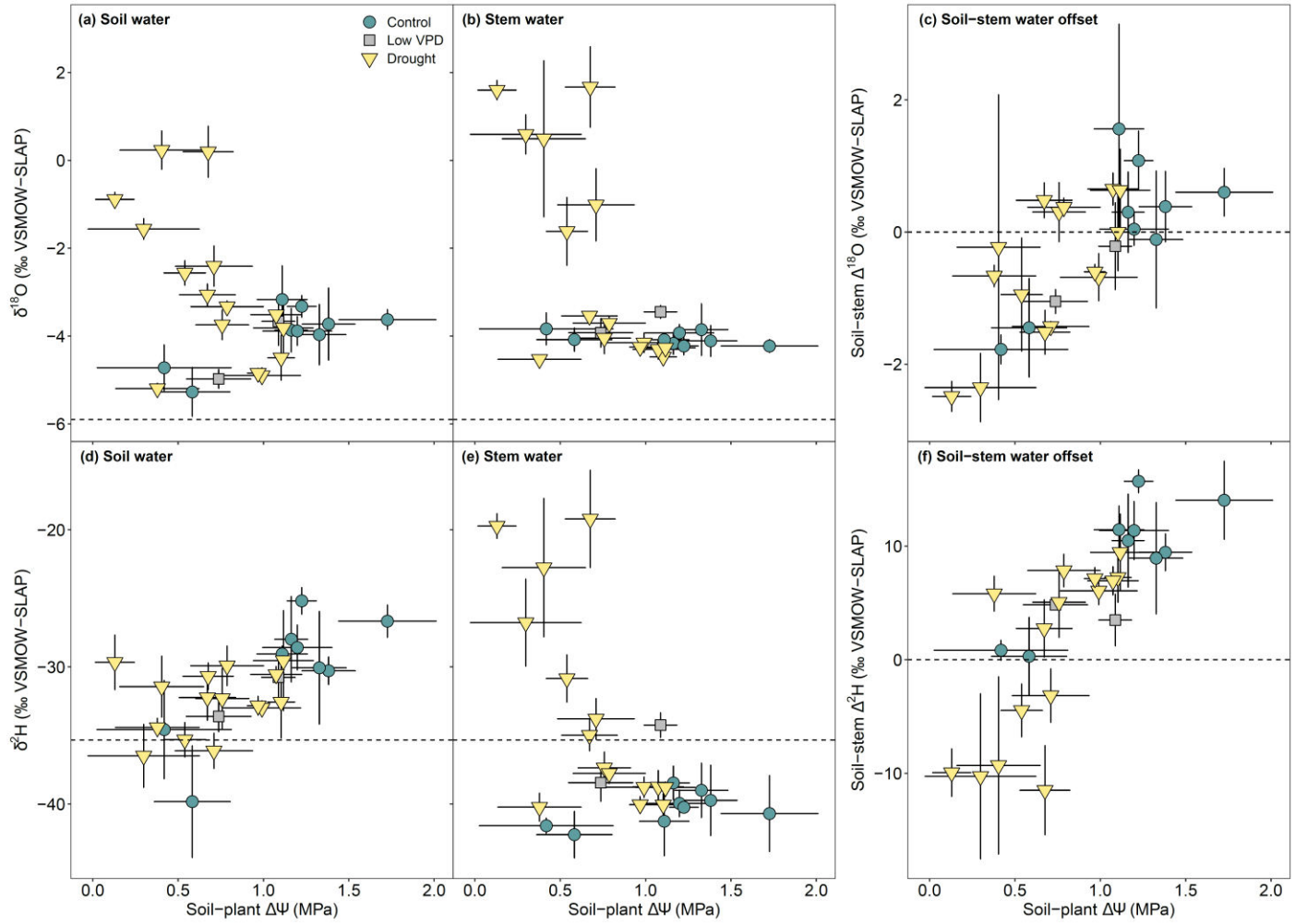
(a) Soil water
(b) Stem water
(c) Soil−stem water offset
(d) Soil water
(e) Stem water
(f) Soil−stem water offset
Control
Low VPD
Drought
δ18O (‰ VSMOW−SLAP)
δ2H (‰ VSMOW−SLAP)
Soil−stem Δ18O (‰ VSMOW−SLAP)
Soil−stem Δ2H (‰ VSMOW−SLAP)
Soil−plant ΔΨ (MPa)
Soil−plant ΔΨ (MPa)
Soil−plant ΔΨ (MPa)

774

775

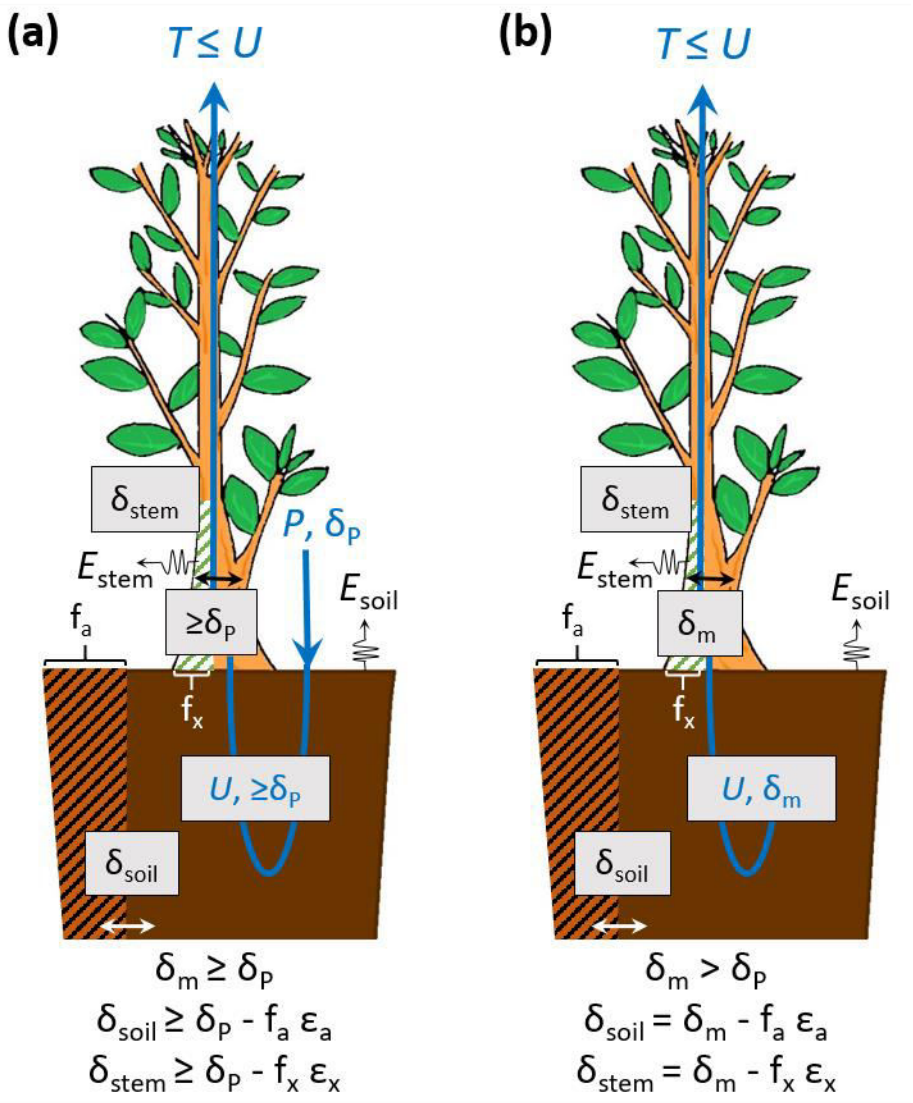
(a)
T ≤ U
δstem
P, δP
Estem
Esoil
fa
≥δP
fx
U, ≥δP
δsoil
δm ≥ δP
δsoil ≥ δP - fa εa
δstem ≥ δP - fx εx
(b)
T ≤ U
δstem
Estem
Esoil
fa
δm
fx
U, δm
δsoil
δm > δP
δsoil = δm - fa εa
δstem = δm - fx εx

***New Phytologist* Supporting Information**

Article title: An explanation for the isotopic offset between soil and stem water in a temperate tree species
Authors: Adrià Barbeta, Teresa E. Gimeno, Laura Clavé, Bastien Fréjaville, Sam P. Jones, Camille Delvigne, Lisa Wingate, Jérôme Ogée
Article acceptance date: Click here to enter a date.

The following Supporting Information is available for this article:

Fig. S1 Soil water retention curves.

Fig. S2 Soil gravimetric water contents and predawn leaf water potentials.

Fig. S3 Midday leaf water potentials and daily amplitude in leaf water potentials.

Fig. S4 Isotopic composition of water pools in the different soils.

Fig. S5 Soil-stem and soil-root isotopic offsets.

Fig. S6 Effect of the low VPD treatment on soil-stem isotopic offsets.

Fig. S7 Effect of leaf stomatal conductance on soil and stem water isotopic compositions.

Fig. S8 Effect of midday leaf water potential on soil and stem water isotopic compositions.

Notes S1 Sensitivity analysis on the control treatment.

Fig. S9 Effect of soil evaporation on the theoretical isotope ratios of soil and stem water.

Fig. S10 Boxplot of the temporal course of soil and plant conditions.

Fig. S11 Boxplot of the temporal course of the isotopic composition of soil and plant water.

Figure S1. Soil water retention curves for three soils used in this experiment. Note the different scales in the x-axis.

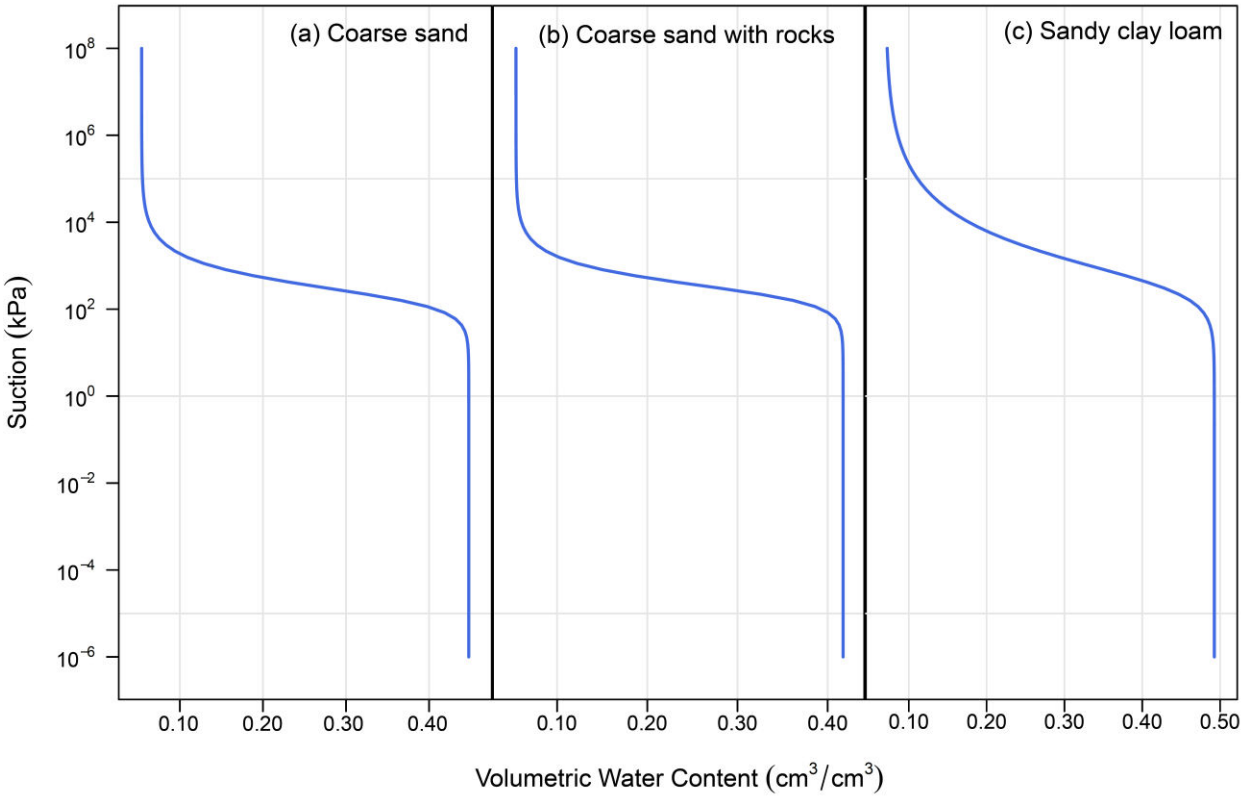

Figure S2. Boxplots of the soil volumetric water content (VWC, a and b) and predawn leaf water potential (Ψ_{pd}, c and d) in control (a and c) and drought-stressed pots (b and d), for each soil type, over the course of the experiment. Boxplots show the interquartile range, the median (black line), the minimum and the maximum values (whiskers) besides outliers (black dots), with N = 10 and 5, for VWC and 5 and 3 for Ψ_{pd}, for drought and control, respectively.

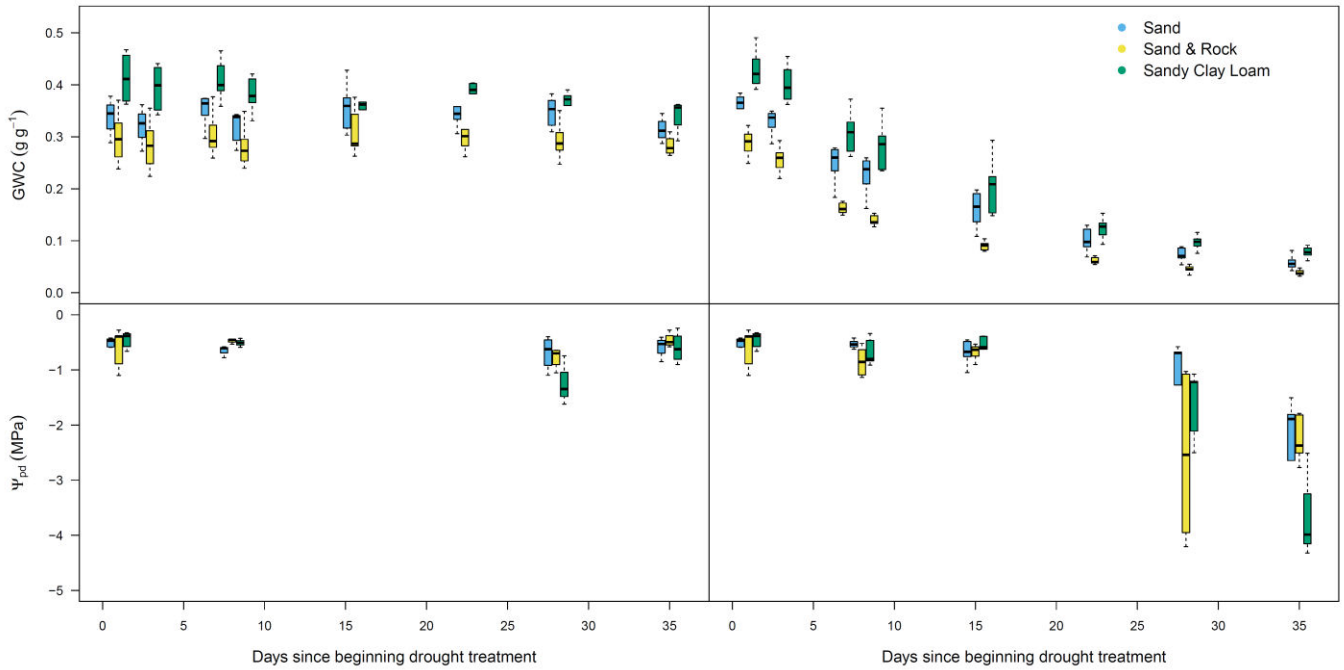

Figure S3. Midday leaf water potential (Ψ_{md}, a and b) and difference between predawn and midday Ψ ($\Delta\Psi_{pd\text{-}md}$, c and d) over the course of the experiment in control (a and c) and drought (b and d) treatments. Boxplots show the interquartile range, the median (black line), the minimum and the maximum values (whiskers) besides outliers (black dots), with $N = 15$ and 9 for drought and control, respectively).

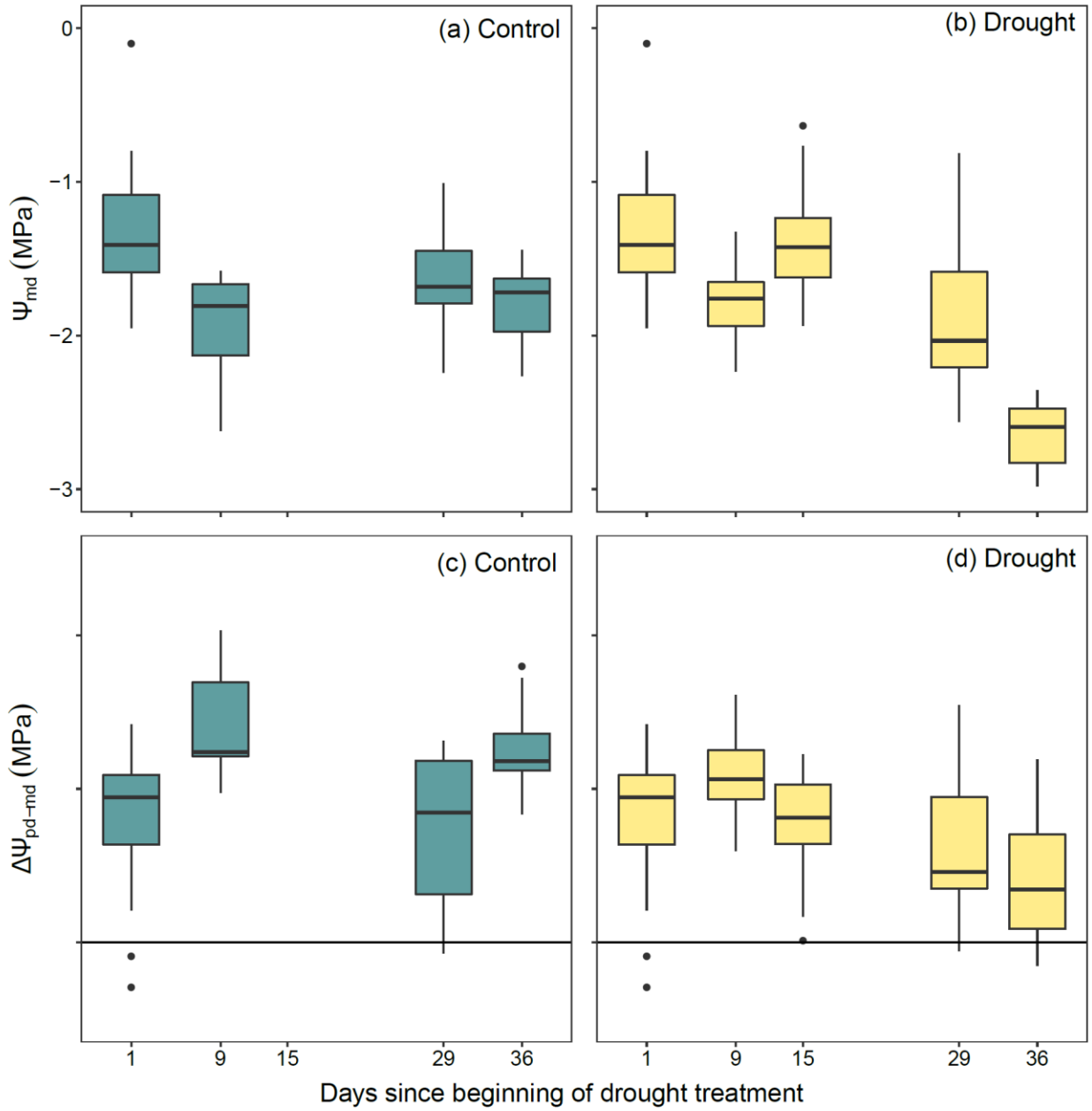

Figure S4. Isotopic composition (δ^2H and $\delta^{18}O$) of soil, stem, root and rock water over the course of the experiment only in the drought treatments pots, and split by soil texture as follows: coarse sand (a, d), coarse sand with rocks (b, e) and sandy clay loam (c, e). The teal line corresponds to the mean of the isotopic composition of the irrigation water and the dashed blue lines are the span of the standard error of the mean. Boxplots show the interquartile range, the median (black line), the minimum and the maximum values (whiskers) besides outliers (black dots), with = 5 and 3, for drought and control, respectively.

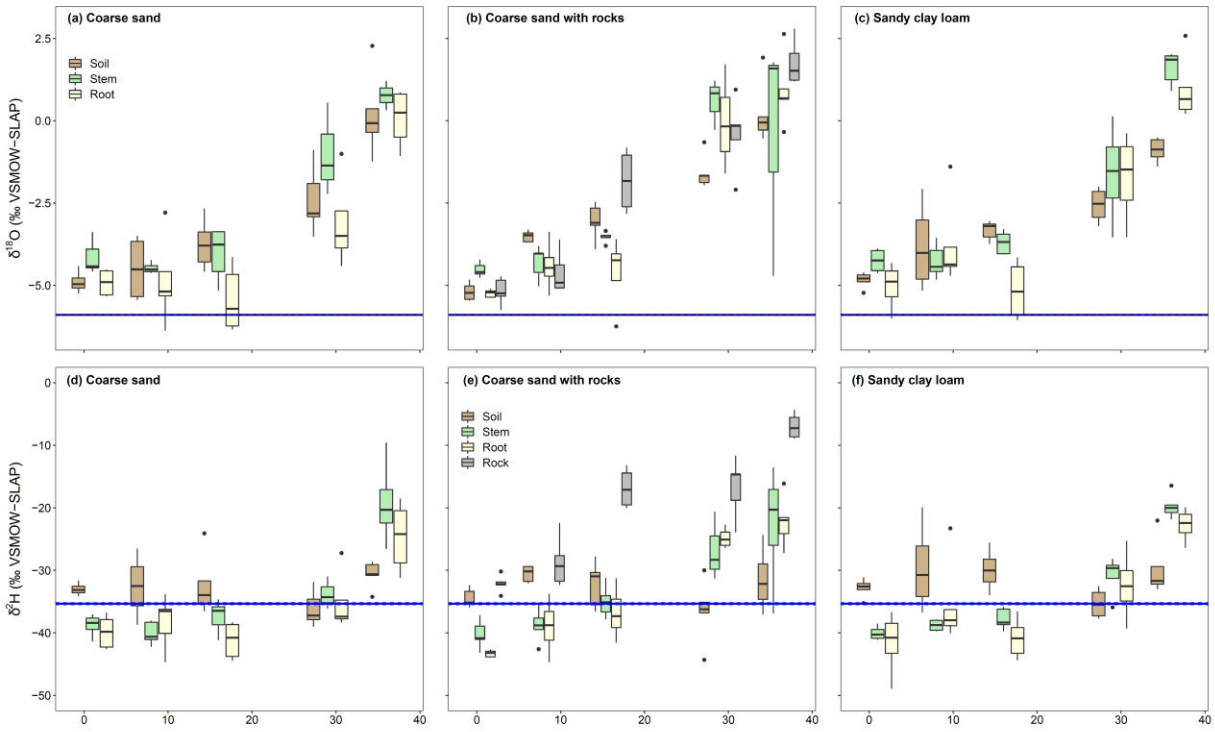

Figure S5. Soil-stem water isotopic offsets ($\Delta^{18}O$ (a) and $\Delta^{2}H$ (c)) over the course of the experiment in control (teal boxes) and drought (yellow boxes) treatment and the same for soil-root isotopic offsets ($\Delta^{18}O$ (b) and $\Delta^{2}H$ (d)). Error bars are the standard error of the mean (*N* = 15 and 9, for control and drought, respectively). Note that control pots were not sampled in the third sampling campaign.

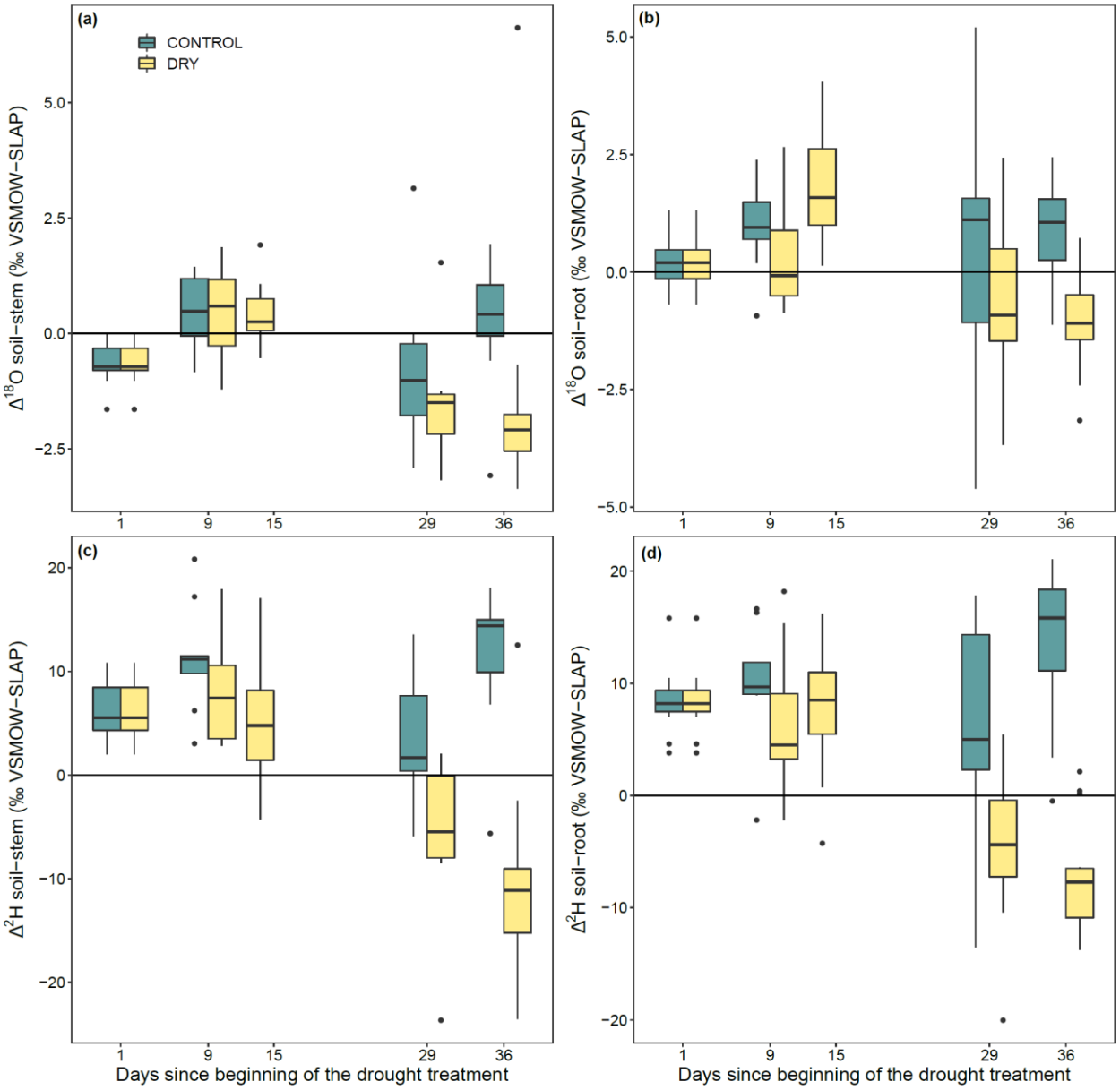

Figure S6. Effect of the VPD treatment (low (blue boxes) or ambient (orange boxes)) on soil-stem isotopic offsets ($\Delta^{18}O$ (a) and $\Delta^{2}H$ (b)). Box heights correspond to the 1^{st}-3^{rd} interquartile, the line inside the box is the value of the median, whiskers correspond to the minimum and maximum values within 1.5 times the interquartile range and data beyond 1.5 times the interquartile range are points outside the whiskers. Significant differences are highlighted with an asterisk (P <0.05).

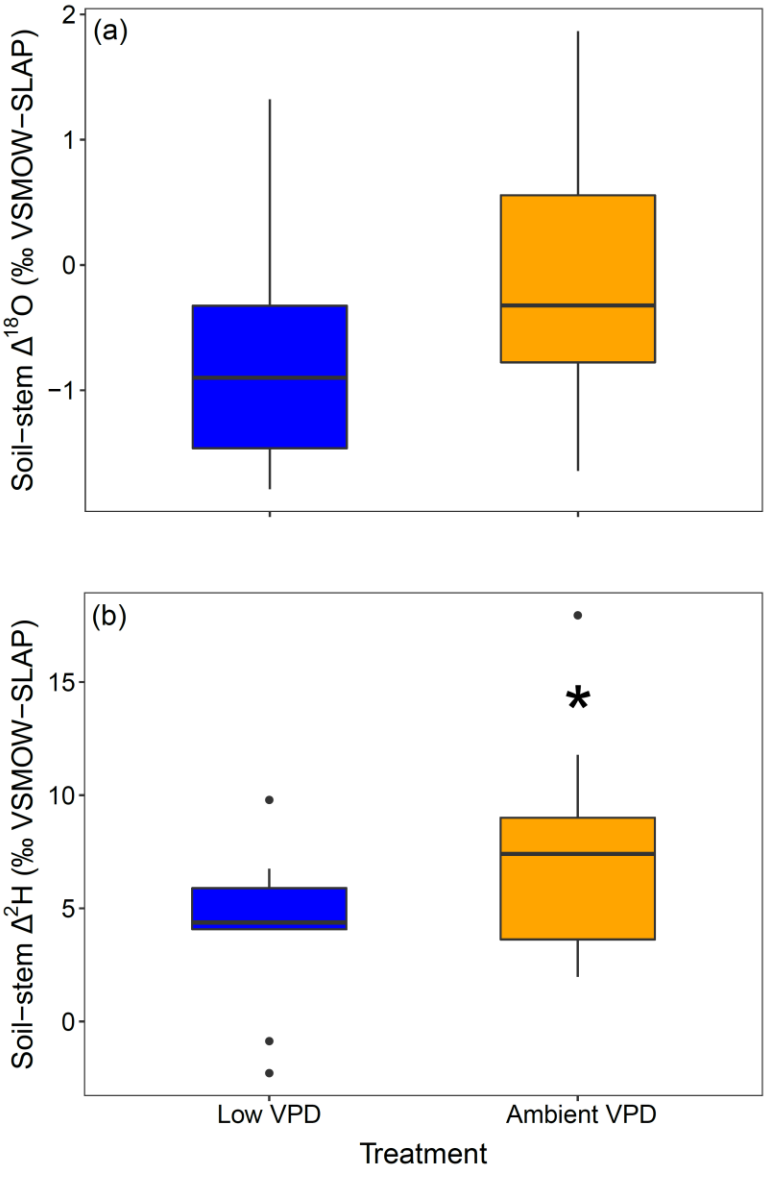

Figure S7. Relationships between the soil and plant isotopic composition ($\delta^{18}O$ (a) and $\delta^{2}H$ (b)) groups of soil, watering and VPD treatments and stomatal conductance at midday. Error bars are standard errors of the mean, and the dashed line indicates the isotopic composition of irrigation water.

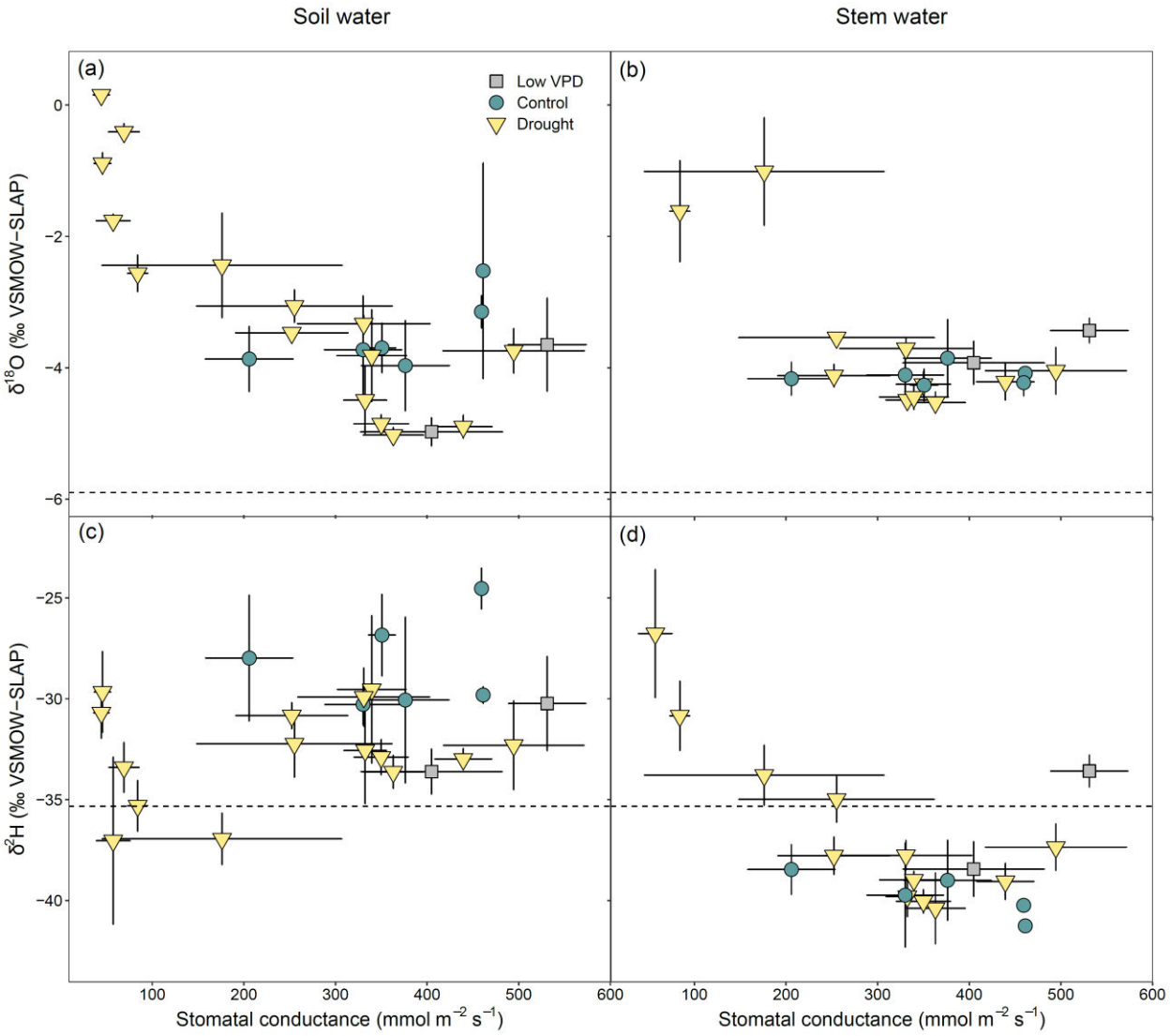

Figure S8. Relationships between the soil and plant isotopic composition groups ($\delta^{18}O$ (a) and $\delta^{2}H$ (b)) of soil, watering and VPD treatments and twig water potentials at midday (Ψ_{md}). Error bars are standard errors of the mean, and the dashed line indicates the isotopic composition of irrigation water.

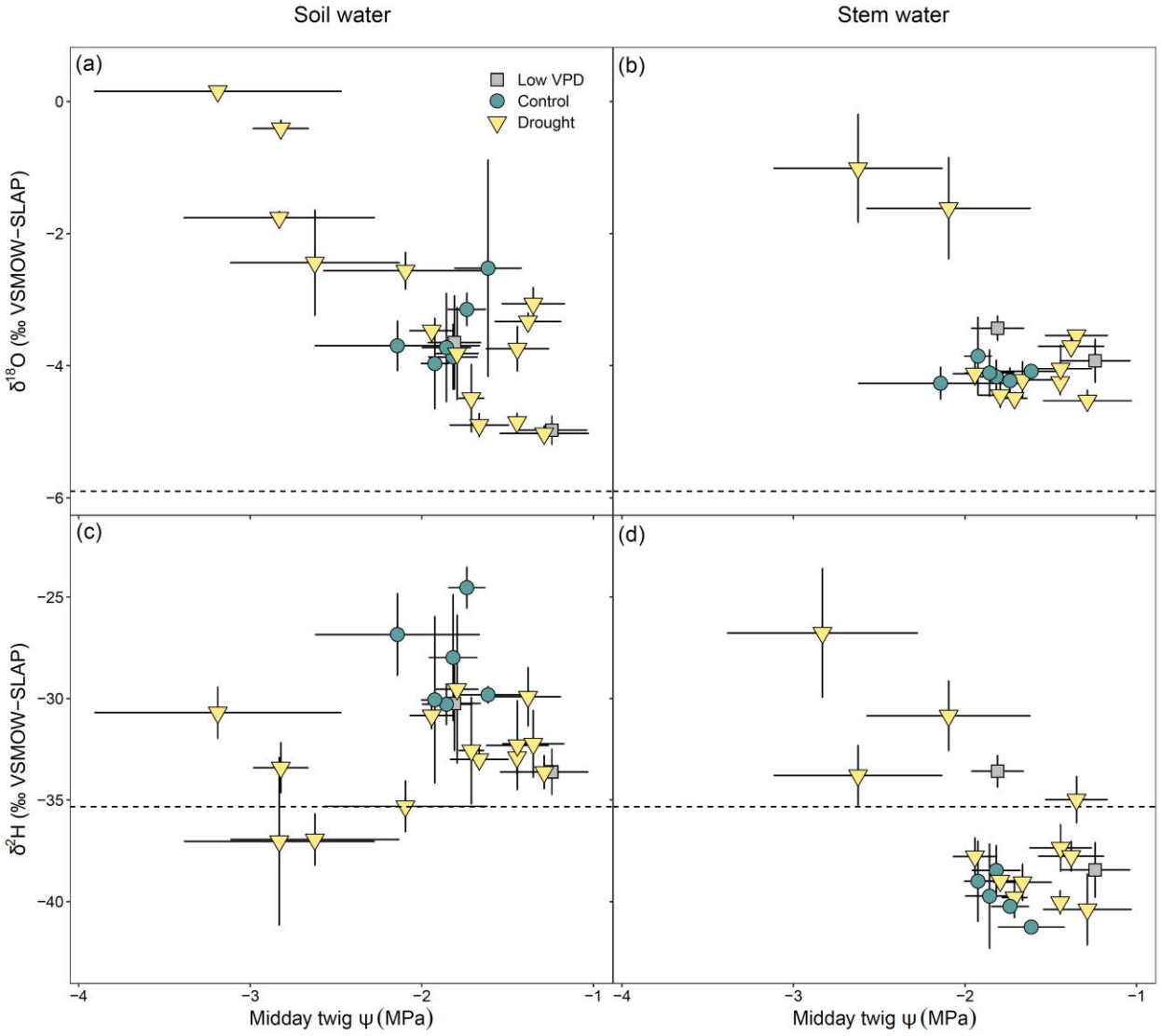

Notes S1. Sensitivity analysis on the control treatment.

In this section, we explore the possible effects of isotopic fractionation during root water uptake and soil evaporation (α_E) on the isotopic composition of soil and stem (xylem) water, under nearly continuous irrigation, transpiration and evaporation. This approximates the situation in our control treatments, whereby evapotranspiration losses were compensated with regular irrigation to ensure that soil moisture content remained the same throughout the experiment.

First we considered the simplest situation where soil evaporation is fully supressed (i.e. the purpose of the plastic covers used to cover the soils in our experiment) and irrigation is added daily to compensate for the soil water taken up by roots (for practical reasons, irrigation was applied only every 3 days in our control treatment but this does not change the reasoning below). In this situation, if there is fractionation during root water uptake (say of 3‰, i.e. with a fractionation factor α_U=0.997<1), then for every day when water is added with an isotope ratio R_P, the same amount is removed by root water uptake with an isotope ratio $\alpha_U R_s < R_s$, where R_s is the isotope ratio of soil water (we neglect possible soil water isotope gradients with soil depth or distance to the rhizosphere for the moment). In other words, transpiration takes relatively fewer heavy water isotopes than there are in the soil, thus soil water becomes enriched in the heavy isotopes, whilst irrigation either enriches or depletes soil water depending if $R_P > R_s$ or not. Over time, the isotope ratio of soil water (R_s) changes until it reaches its steady-state (s.s.) value: R_s(s.s.) = R_P/α_U. In this situation, both fluxes into and out of the soil have the same isotopic signature because irrigation adds water to the soil with the composition R_P and root uptake removes water from the soil with a composition $\alpha_U R_s$(s.s.) = R_P. When the isotopic steady state is reached soil water will have an isotope ratio R_P/α_U that is more enriched than irrigation water (by 3‰ in our example). During all this time, stem (xylem) water had the same isotope composition as root water uptake, i.e., $R_x = \alpha_U R_s$, which is (over time) above or below R_P depending on the initial value of R_s compared to R_P. However once isotopic steady state is reached, R_x reaches R_x(s.s.) = $\alpha_U R_s$(s.s.) = R_P, regardless of the initial value of R_s. In other words, at isotopic steady state, we should expect the isotope ratio of the stem (xylem) water to be the same as irrigation water, and soil water to be more enriched than

irrigation water to an extent that reflects the isotope fractionation during root water uptake α_U. By no means, should we expect stem (xylem) water to become depleted in heavy isotopes compared to irrigation water.

The simple example above was derived assuming no soil evaporation. However, if soil evaporation is not completely suppressed, then this should create an isotopic enrichment of soil water different from the situation above and could also enrich stem (xylem) water. A mathematical treatment of this situation is therefore required. In the situation where water is removed from the soil by root uptake and soil evaporation, the soil water mass balance becomes:

$$\frac{dW}{dt} = P \quad E \quad U \quad 0 \tag{S1}$$

In this equation, P, E and U (in L of water per day) represent the rates of irrigation, soil evaporation and root water uptake, respectively, W is the soil water content (in L) and t is time (in days). A similar mass balance equation can also be written for the heavy isotope species (either $^1H_2{}^{18}O$ or $^1H^2H^{16}O$):

$$\frac{dWR_S}{dt} = PR_P \quad ER_E \quad UR_U \quad W\frac{dR_S}{dt} \tag{S2}$$

In this equation, R_S, R_P, R_E and R_U are the isotope ratios of bulk soil water, irrigation water, soil evaporation and root water uptake, respectively. The second equality in Eq. S2 was obtained by decomposing the derivative of the product WR_S and noting that, according to Eq. S1, $dW/dt = 0$. In the following, we will express R_E and R_U with respect to R_s and introduce isotope fractionations: $R_E = \alpha_E R_s$ and $R_U = \alpha_U R_s$. We will also express E as a fraction of the root water uptake rate U: $E = f_E U$. (This notation does not imply any functional relationship between E and U but is there only to quantify the relative proportion of soil evaporation compared to root uptake). With this notation, Eq. S1 simplifies to $P = (1 + f_E)U$ and Eq. S2 can be re-arranged as:

$$\frac{dR_S}{dt} + \frac{_U P}{W}\frac{1 + _E/_U f_E}{1 + f_E}R_s = \frac{P}{W}R_P \tag{S3}$$

At isotopic steady state, $dR_s/dt = 0$ and we obtain:

$$R_s(s.s.) = \frac{1 + f_E}{1 + {}_E/{}_U f_E} \frac{R_P}{{}_U} \quad \text{(S4)}$$

If $f_E = 0$ we have the situation described above where evaporation is totally suppressed and $R_s(s.s.) = R_P/\alpha_U$. If $f_E \neq 0$, then soil water will become even more enriched than R_P/α_U if $\alpha_E/\alpha_U < 1$ but it can also become less enriched if $\alpha_E/\alpha_U > 1$. Note that, because both evaporation and root uptake are supposed to enrich soil water, α_E and α_U are both smaller than unity. Therefore, $\alpha_E/\alpha_U > 1$ means that the isotopic enrichment of soil water caused by soil evaporation is smaller than the isotopic enrichment caused by root uptake. This is why the overall effect in this situation is to have a soil water pool that is less enriched than if root uptake was the only enriching process.

Equation S3 is also instructive because it gives an indication of the time constant required to reach isotopic equilibrium: $\tau \approx W/P$. With P = 0.06 L/day (this is coherent with our irrigation records and with Fig. S2b that shows that about 0.2 L L^{-1} is lost in about 10 days at the beginning of the drought treatment for a total soil volume of about 3L) and W = 1.5 L (i.e. 3L of soil with a water content of about 0.5 L L^{-1}, see Fig. S2a), we obtain $\tau \approx$ 25 days. This means that it takes about 1-2 months to reach isotopic steady state, approximately the duration of the irrigation period prior to our first sampling campaign (i.e. from February to mid-May 2018). Therefore, we should expect that isotopic steady state was attained by the time of our first sampling campaign.

Equation S4 has been derived by replacing R_E by $\alpha_E R_s$ but α_E is not independent of α_U and f_E (and all other variables affecting the isotopic composition of soil water at the evaporation site). Indeed, the isotope ratio of soil evaporation (R_E) is related to that of soil water at the evaporation site (R_{es}) and also to the isotope ratio of atmospheric vapour at the soil surface (R_v) (Barnes & Allison, 1983; Farquhar *et al.*, 2007):

$$R_E = \frac{R_{es}/{}_{lv} \quad hR_v}{(1 \quad h){}_k} \quad \text{(S5)}$$

where h denotes air relative humidity at the soil surface and α_{lv} and α_k are the isotopic fractionations during liquid-vapour transition and water vapour diffusion from the evaporation

site to the soil surface, respectively. α_{lv} is only a function of soil temperature while α_k depends on the intensity of the airflow above the soil surface.

Because of isotope fractionations associated with soil evaporation and root uptake, the isotope ratio of soil water is not uniform, so that $R_{es} \neq R_s$, even if root water uptake is uniform throughout the soil profile. The isotope ratio of water vapour at the soil surface will also depend on the ratio of evaporation and transpiration (f_E), and water vapour exchange between the glasshouse atmosphere and the air underneath the plastic plate that covers the soil. If this exchange is slow we could assume that most of the water vapour at the soil surface comes from soil evaporation, so that $R_v = R_E$. In this situation, Eq. S5 can be re-arranged:

$$R_E = \frac{R_{es}}{{}_{lv}h + (1 \quad h)\ {}_{lv} \quad {}_k} \tag{S6}$$

We can also define $Z(\alpha_U, f_E) = R_{es}/R_s$ so that:

$${}_E = \frac{Z(\quad {}_U, f_E)}{{}_{lv}h + (1 \quad h)\ {}_{lv} \quad {}_k} \tag{S7}$$

To a good approximation, we can assume that in our control treatment, the soil column stays near saturation and we can neglect water vapour fluxes compared to liquid water fluxes. We also assume the soil column to be isothermal and root uptake to be uniform throughout the soil profile. In this situation, at steady state, the liquid water flux varies linearly with soil depth (z) from $(P - E)/(A\rho_w) = U/(A\rho_w) = q_{l0}$ at the soil surface ($z = 0$) to zero at the bottom ($z = z_{max}$): $q_l = q_{l0}(1 - z/z_{max})$. We normalised the fluxes P, E and U (in L/day or kg/s) by the soil area (A) and water density (ρ_w) to make sure that q_{l0} has the dimension of a velocity (m/s).

At isotopic steady state, the isotope ratio of soil water satisfies the following ordinary differential equation (see for example equation 11 of Haverd & Cuntz, 2010):

$$D_{l,iso}\frac{d^2R}{dz^2} \quad q_{l0}\left(1 \quad z/z_{max}\right)\frac{dR}{dz} + \frac{q_{l0}}{z_{max}}\left(1 \quad {}_U\right)R = 0 \tag{S8}$$

The water isotope flux at the bottom of the soil column is zero (as for the total water flux q_l) and the flux at the soil surface is given by $q_P R_P - q_E R_E$ where $q_P = P/(A\rho_w) = q_{l0}(1 + f_E)$ and $q_E = E/(A\rho_w) = q_{l0} f_E$.

Because $q_{l,iso} = q_l R - D_{l,iso}(dR/dz)$, these boundary conditions lead to:

$$\begin{cases} \left.\frac{dR}{dz}\right|_{z=z_{max}} = 0 \\ q_{l0}R(0) \quad D_{l,iso}\left.\frac{dR}{dz}\right|_{z=0} = q_P R_P \quad q_E R_E \end{cases} \tag{S9}$$

Defining $x = 1 - z/z_{max}$, $P_l = q_{l0} z_{max}/D_{l,iso}$, and $y(x) = R(z)$, Eq. S8 can be re-arranged:

$$\frac{d^2y}{dx^2} + P_l x \frac{dy}{dx} + P_l\left(1 \quad _U\right) y = 0 \tag{S10}$$

Making use of Eq. S6 and noting that $R_{es} = R(0) = y(1)$, the boundary conditions (Eq. S9) become, with these new notations:

$$\begin{cases} \left.\frac{dy}{dx}\right|_{x=0} = 0 \\ \frac{1}{P_l}\left.\frac{dy}{dx}\right|_{x=1} + \left[1 + f_E \frac{1}{_{lv}h + (1 \quad h)\ _{lv} \quad _k}\right] y(1) = \left(1 + f_E\right) R_P \end{cases} \tag{S11}$$

A solution of Eq. S10 with the boundary condition at $x = 0$ is provided by Farquhar and Gan (2003) and is a confluent hypergeometric series of the first kind, or Kummer function ${}_1F_1(a, b, x)$:

$$y(x) = a_0 \cdot {}_1F_1\left(\frac{1 \quad _U}{2}, \frac{1}{2}, \frac{P_l}{2}x^2\right) \tag{S12}$$

The constant a_0 is obtained using the second boundary condition, knowing that:

$$\frac{d}{dx}\left\{{}_1F_1\left(a, b, \ 0.5P_l x^2\right)\right\} = \frac{a}{b} P_l \times \left\{{}_1F_1\left(a+1, b+1, \ 0.5P_l x^2\right)\right\} \tag{S13}$$

This gives:

$$a_0 = \frac{R_P\left(1 + f_E\right)}{(\ _U \quad 1) \times {}_1F_1\left(0.5(2 \quad _U), 1.5, \ 0.5P_l\right) + \left(1 + f_E / \ _{es}\right) \times {}_1F_1\left(0.5(1 \quad _U), 0.5, \ 0.5P_l\right)} \tag{S14}$$

where $\alpha_{es} = \alpha_{lv} h + (1\text{-}h)\alpha_{lw}\alpha_k$. From Eqs. S12 and S14 we can compute $R_{es} = R(0) = y(1)$ for any values of α_U and f_E.

Integrating Eq. S10 between 0 and 1 also gives:

$$R_s = \int_0^1 y\,dx = \frac{1}{\alpha_U}\left[R_P(1+f_E) \quad R_{es}\frac{f_E}{\alpha_{es}} \right] \tag{S15}$$

We will note that Eq. S15 is simply a re-arrangement of Eq. S4 where $\alpha_E = R_E/R_s$ has been replaced by $(R_{es}/\alpha_{es})/R_s$. From Eq. S15 we can compute $Z(\alpha_U, f_E) = R_{es}/R_s$ and finally α_E, but this extra step is a bit unnecessary if we are only interested in R_s, R_{es} and eventually $R_x = R_U = \alpha_U R_s$ because all these quantities can be computed from Eqs. (S12-S15).

Steady-state values of R_s, R_x and R_{es} are shown in Fig. S9 as a function of f_E and for different values of $\varepsilon_U = \alpha_U - 1$. We assumed a soil surface area of 10 cm^2 (leading to $q_P \approx 70$ µm/s), a maximum soil depth of 35 cm (leading to a soil volume of 3.5 L) and air temperature and relative humidity of 27°C and 70%, respectively. We also indicated the range of values for R_s and R_x that we observed in our control experiment (see Fig. 3 in the main text).

First, we can see that when $f_E = 0$, $R_x = R_p$ and $R_s = R_p/\alpha_U$, as already predicted by Eq. S4, and also $R_{es} = R_s$. When $f_E > 0$ R_x becomes slightly more enriched than R_p, but increasing fractionation during root uptake (i.e. taking more negative ε_U values) does not affect R_x but only enriches R_s above R_x by about $-\varepsilon_U$. For $f_E \approx 0.05$-0.1 and $\alpha_U = 1$, our predictions for R_s match well the observations for both $^2H/^1H$ and $^{18}O/^{16}O$ ratios, supporting the idea that no fractionation during root water uptake occurred. Our predictions for R_x at $f_E \approx 0.05$-0.1 also match well our observations, but only for oxygen isotopes. For hydrogen isotopes, our observations of bulk stem (xylem) water cannot be explained by any combination of f_E and α_U. We conclude from this analysis that, if soil evaporation was probably not completely suppressed in our control treatment($f_E \approx 0.05$-0.1), fractionation during root water uptake does not seem to have occurred ($\alpha_U = 1$) thus another fractionation process must be responsible for the observed depletion of bulk stem water compared to soil water in the control treatment. Isotopic heterogeneity between vessel water (with isotope ratio $\alpha_U R_s = R_s$) and other xylem tissues could explain such depletion if xylem tissues were depleted compared to vessel water.

Figure S9. Isotope ratios R_{es}, R_s and R_x, expressed as enrichment above irrigation water R_p, and computed using Eqs. S13 and S15 for different values of f_E and α_U. Observed ranges are also indicated.

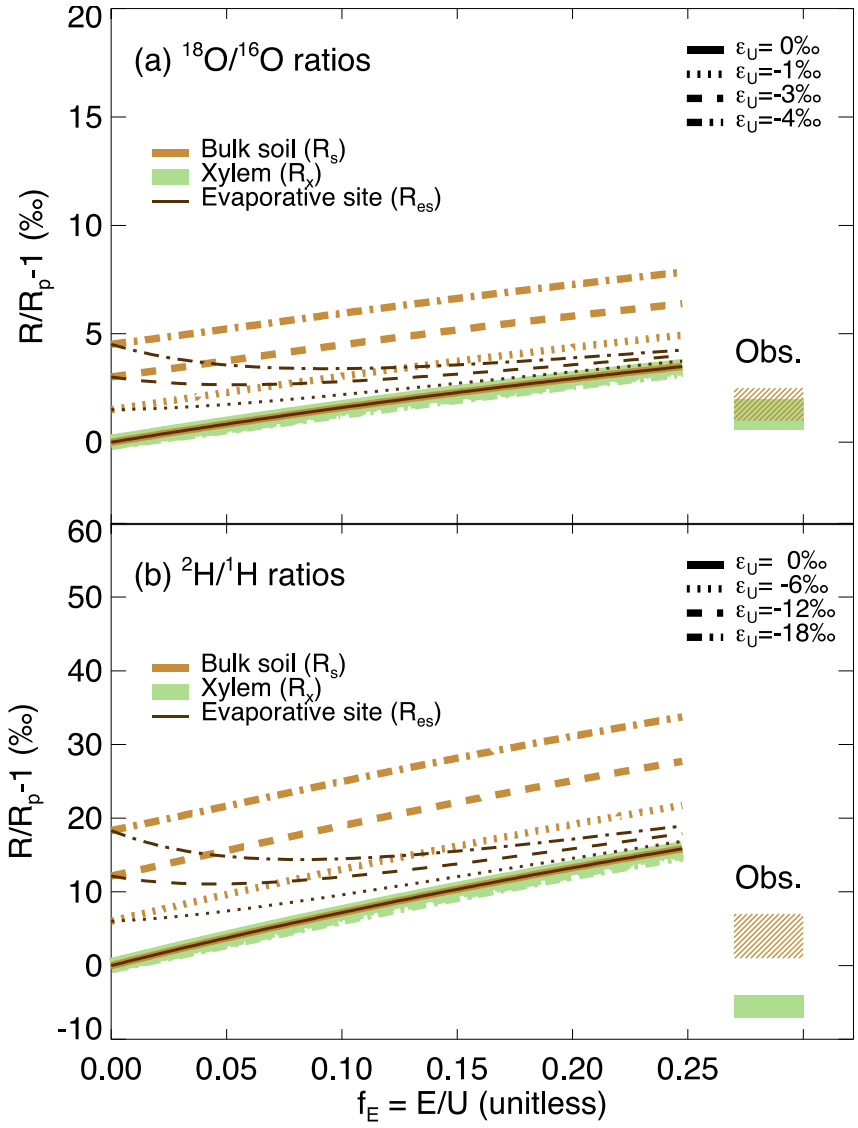

Figure S10. Boxplots of the soil gravimetric water content (GWC, a and b), predawn leaf water potential (Ψ_{pd}, c and d), plant water content (e and f) and stomatal conductance (g and h) in control (a, c, e and g) and drought-stressed pots (b, d, f and h). Boxplots show the interquartile range, the median (black line), the minimum and the maximum values (whiskers) besides outliers (black dots), with N = 10 and 5, for GWC and plant water content, and N=5 and 3 for Ψ_{pd} and stomatal conductance, for drought and control, respectively.

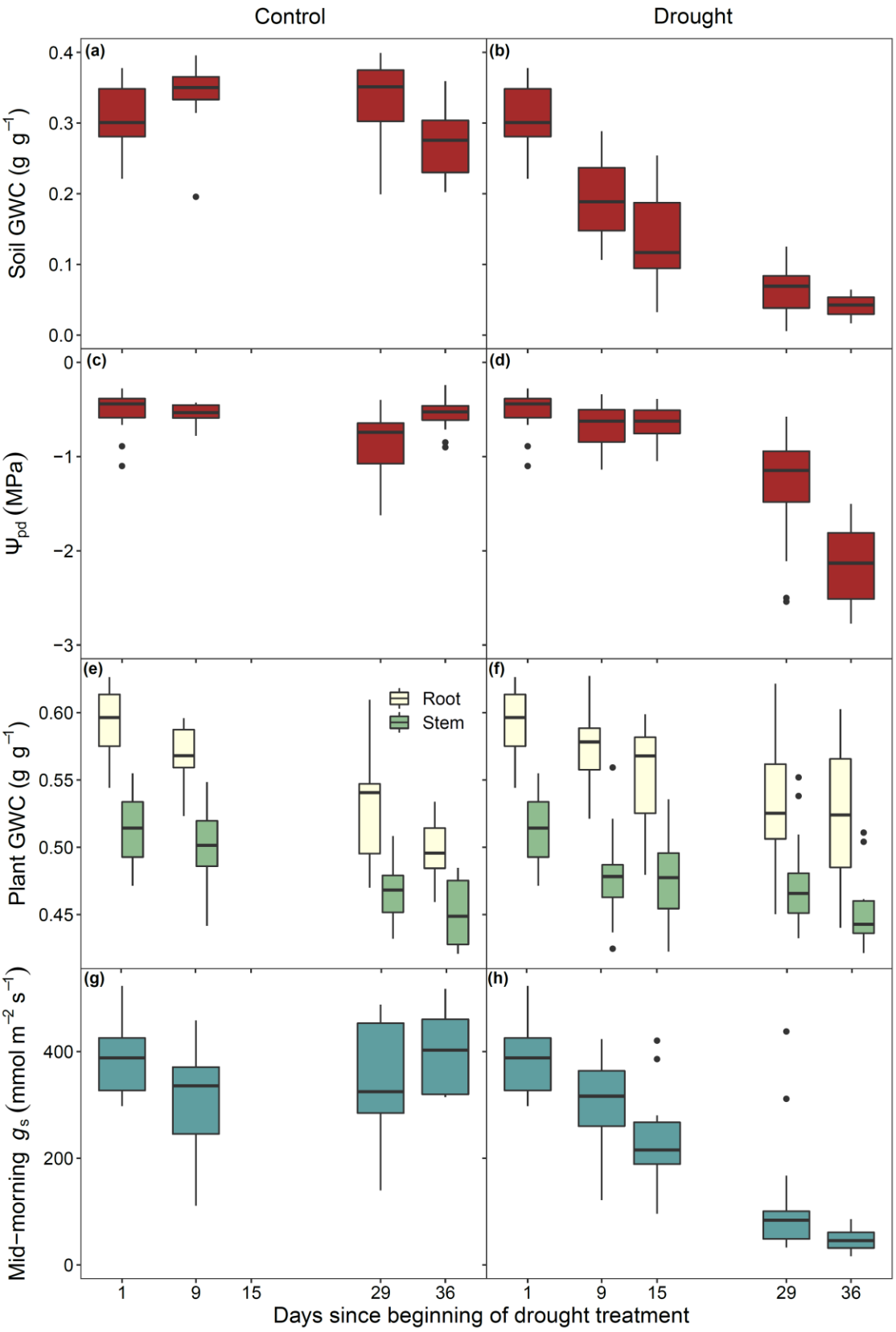
Control
Drought
(a)
(b)
(c)
(d)
(e)
(f)
(g)
(h)
Soil GWC (g g^{-1})
Ψ_{pd} (MPa)
Plant GWC (g g^{-1})
Mid−morning g_s (mmol m^{-2} s^{-1})
Root
Stem
0.4
0.3
0.2
0.1
0.0
0
−1
−2
−3
0.60
0.55
0.50
0.45
400
200
0
1
9
15
29
36
Days since beginning of drought treatment

Figure S11. Boxplots of the isotopic composition of soil, root and stem water in control (a, c) and drought-stressed pots (b, d). Boxplots show the interquartile range, the median (black line), the minimum and the maximum values (whiskers) besides outliers (black dots), with N = 15 and 9 for drought and control, respectively.

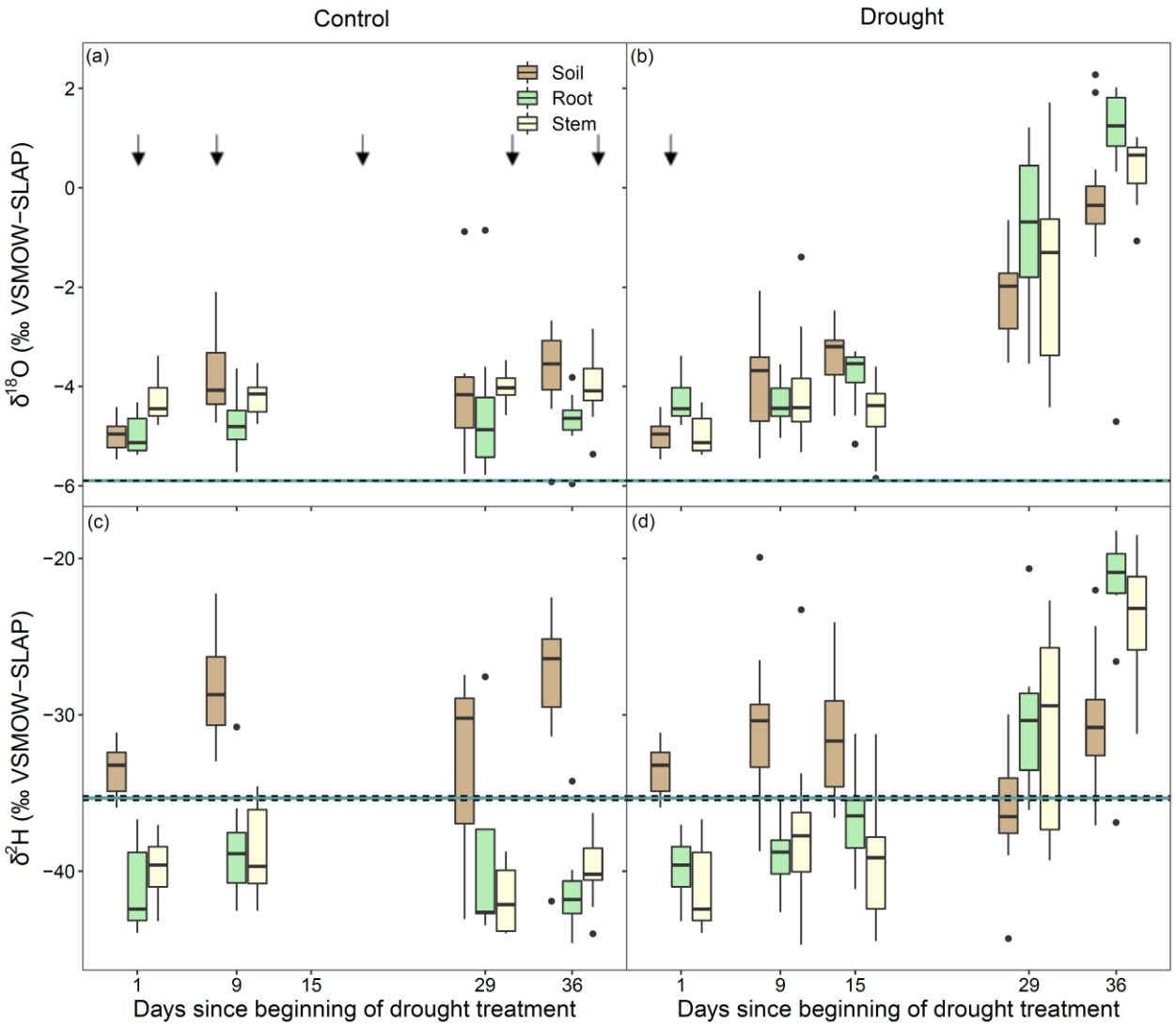

References

Barnes C, Allison GB. **1983**. The distribution of deuterium and ^{18}O in dry soils .1. Theory. *Journal of Hydrology* **60**: 141–156.

Farquhar GD, Gan K. **2003**. On the progressive enrichment of the oxygen isotopic composition

of water along a leaf. *Plant Cell and Environment* **26**: 801–819.

Farquhar GD, Cernusak LA, Barnes B. **2007**. Heavy Water Fractionation during Transpiration. *Plant Physiology* **143**: 11–18.

Haverd V, Cuntz M. **2010**. Soil–Litter–Iso: A one-dimensional model for coupled transport of heat, water and stable isotopes in soil with a litter layer and root extraction. *Journal of Hydrology* **388**: 438–455.